OPTICAL AND INFRARED MASERS

17th, 18th and 19th Semi-Annual Status Reports

for period

April 1, 1971 to September 30, 1971
October 1, 1971 to March 31, 1972
April 1, 1972 to September 30, 1972

To:

National Aeronautics and Space Administration
Goddard Space Flight Center
Greenbelt, Maryland 20771

NASA Research Grant NGL 22-009-012

M.I.T. Project DSR 76148

From:

Department of Physics
Massachusetts Institute of Technology
Cambridge, Massachusetts 02139

Issue Date: July 13th, 1973

TABLE OF CONTENTS

This progress report summarizes the ongoing research of the Massachusetts Institute of Technology Laser and Quantum Electronics Group under NASA Research Grant NGL 22-009-012, performed during the periods April 1, 1971 to September 30, 1971; October 1, 1971 to March 31, 1972 and April 1, 1972 to September 30, 1972.

Appendices (cont'd.)

C. Anisotropic Ultrahigh Gain Emission Observed in Rotational Transitions in Optically Pumped HF Gas

D. Selective Reabsorption Leading to Multiple Oscillations in the 8446Å Atomic Oxygen Laser

E. Interactions Among Multiple Lines in the 8446Å Atomic-Oxygen Laser

I. Tunable Infrared Light Sources and Applications

A number of methods are being pursued to generate tunable coherent radiation in the infrared for spectroscopic and other applications. Our recent experiments have shown that metal-to-metal point contact diodes can be used to generate microwave sidebands on infrared laser radiation.[1] In these experiments, a laser and a microwave source are mixed in the point contact diode, and sum and difference frequencies are detected in the reradiated signal. Although sufficient for some spectroscopic applications, the conversion efficiency is as yet rather small ($\sim 10^{-10}$). Modulation with an electro-optic modulator (GaAs) promises to produce conversion efficiencies of 10^{-5} or greater. A modulator for producing 600 MHz sidebands has been built and is being tested, and one for 20 GHz is being designed. These frequency ranges are of particular interest for some precision spectroscopy of high lying states in singly ionized He in the 10μ region. The experiments make use of the nonlinear saturation which occurs at the center of a Doppler broadened atomic or molecular line when a standing wave field is tuned to resonance and thus require sufficient power to saturate the transition.

In addition, a spin flip Ramam laser is under construction for similar experiments in hydrogen, utilizing a CO laser pump in the 5μ region. The system is being designed for maximum stability, in order to produce a spin flin laser which can be used for high precision measurements.

II. Precision Frequency and Wavelength Measurements in the Infrared with Applications to Atomic Clocks

The development of techniques for comparing widely differing laser frequencies by means of harmonic mixing in a metal-to-metal point contact diode has permitted the absolute measurement of frequencies down to the near infrared. In the last progress report, methods for constructing a phase-locked frequency multiplier chain which would be capable of transferring the accuracy of the cesium frequency standard to an infrared transition were described. Such a frequency multiplier chain, utilizing tunable microwave sidebands to offset laser drift, is under construction for the purpose of measuring the frequency of stabilized CO_2 laser transitions, which promise to be convenient frequency standards in the infrared.

The laser stabilization is performed using the narrow nonlinear resonance observed in the 4.3μ fluorescence from a CO_2 sample cell when a standing wave field is tuned to the center of the Doppler line. A second CO_2 laser and stabilization system have been constructed in order to test the stability and resetability of the system. In this system, a larger beam size and higher power have been used in order to decrease transit time broadening and to increase the signal to noise. It is hoped in this way to considerably improve upon the one part in 10^8 stability achieved with the previous system. It is also planned to investigate the pressure shifts in CO_2 for the purpose of establishing the absolute accuracy of this stabilization method for CO_2 lasers.

III. Zero-Degree Pulse Propagation in a Resonant Medium

In the area of short pulse interactions, it was decided to discontinue attempts at studying adiabatic rapid passage because of insufficient signal to noise. Emphasis has shifted to the generation of zero-degree optical pulses and the study of their propagation through a resonant medium. Such pulses result if a 180° phase change is produced in the center of the pulse so that the integral of the electric field is zero. The second part of the pulse is consequently in amplifying phase, and extracts the energy from the medium absorbed from the first part of the pulse. A zero-degree pulse thus propagates with reduced loss due to resonant absorption.

A GaAs electro-optic modulator has been used to generate successive 2-or 6-nsec pulses with or without a phase change between them, utilizing the output of a CO_2 or N_2O laser. The propagation of these pulses through a resonant CO_2 or NH_3 absorber has been studied in the linear absorption regime, where the absorption coefficient and pulse evolution can be calculated using Fourier techniques. It is planned to extend these measurements to the nonlinear regime where detailed calculations of the pulse evolution are not available. A paper describing this work which has been published in Applied Physics Letters[2] is included as Appendix A.

IV. Observation of Dicke Superradiance in Optically Pumped HF Gas

The first observations of the evolution of an initially inverted atomic system into a coherently radiating superradiant state, as proposed originally by Dicke, have been made in optically pumped HF. Pumping on a vibrational transition produces complete inversion on a coupled rotational transition. The system is observed to emit a short duration pulse considerably delayed from the excitation pulse, even with neglible feedback. The high gain allows operation at very low pressures (~mTorr) where relaxation times are long. Observed pulse delays and ringing are in agreement with theoretical calculations. This work has recently appeared in publication[3] and is described in more detail in Appendix B.

V. Unidirectional Laser Amplifier with a Built-in Isolator

The laser-induced line narrowing effect has been used to produce a unidirectional laser amplifier in optically pumped HF gas.[4] Because of its high gain, HF proved to be a more suitable system than optically pumped NH_3, which was previously tried. This type of laser has the unique property that if the pump laser is detuned from the center of the Doppler line, in a ring laser cavity, the system can exhibit gain on one side of a Doppler broadened line and loss on the other. A feedback signal is thereby attenuated rather than amplified, and the laser is effectively isolated from its surroundings. These experiments are described in more detail in Appendix C.

VI. Progress in Infrared Metal-to-Metal Point-Contact Tunneling Diodes

Considerable progress has been made to explore further application of our infrared metal-to-metal point-contact tunneling diode. Among these, the diode's properties as a generator of radiation at the synthesized frequencies of two applied fields have been used to obtain detailed information on its I-V characteristics at infrared frequencies. In the experiment, the diode is subjected simultaneously to the output of a CO_2 laser radiation and a microwave klystron radiation. The radiation emitted from the diode at new frequencies consisting of the first and second microwave side-bands of the 10.6μ CO_2 laser radiation is detected by means of a He-cooled Cu:Ge detector. The dependence of the emitted radiation versus a bias field applied to the point-contact diode is studied in detail. The results are compared with a theoretical model in which electron tunneling across a thin oxide layer existing at the point contact is assumed to be responsible for the nonlinear I-V characteristics. This analysis has provided a great deal of information on the tunneling barrier, including its height, shape and width. We are now proceeding to explore a variety of possibilities to improve upon conversion efficiency of the diode. Furthermore, the method described in the above experiment is being explored for application as a tunable frequency radiation, in which frequency tunability is achieved by means of microwave frequency tuning.

VII. Laser Studies of Atomic Oxygen

A series of laser studies in atomic oxygen have now been completed.[5,6] The results are included as Appendices D and E.

REFERENCES

1. A. Sanchez, S. K. Singh and A. Javan, Appl. Phys. Lett. 21, 240 (1972).

2. H. P. Grieneisen, J. Goldhar, N. A. Kurnit, A. Javan and H. R. Schlossberg, Appl. Phys. Lett. 21, 559 (1972).

3. N. Skribanowitz, I. P. Herman, J. C. MacGillivray and M. S. Feld, Phys. Rev. Lett. 30, 309 (1973).

4. N. Skribanowitz, I. P. Herman, R. M. Osgood, Jr., M. S. Feld and A. Javan, Appl. Phys. Lett. 20, 428 (1972).

5. M. S. Feld, B. J. Feldman, A. Javan and L. H. Domash, Phys. Rev. A7, 257 (1973).

6. L. H. Domash, B. J. Feldman and M. S. Feld, Phys. Rev. A7, 262 (1973).

APPENDIX A

OBSERVATION OF THE TRANSPARENCY OF A RESONANT MEDIUM TO ZERO-DEGREE OPTICAL PULSES

H.-P. Grieneisen,[+] J. Goldhar,[++] N. A. Kurnit, A. Javan and H. R. Schlossberg

ABSTRACT

Experiments are described in which low intensity laser pulses of zero area ($\int_{-\infty}^{\infty} \mathcal{E}(z,t)dt=0$) are propagated through a degenerate resonantly absorbing medium with greatly reduced absorption. These pulses are constructed either electro-optically or by allowing a nonzero-degree pulse to evolve toward zero area by means of a resonant absorption and reradiation process. We observe the transmission of as much as 65% of the energy of such pulses through a resonant absorber which attenuates the same c.w. laser by $e^{-\alpha L}$, with $\alpha L \approx 20$.

[+] On leave from Universidade Federal do Rio Grande do Sul, Porto Alegre, Brazil. Work done with partial support from Conselho Nacional de Pesquisas, Brazil.

[++] Hertz Foundation Predoctoral Fellow.

The transparency of a resonant absorber to pulses of large "area" $\theta=2n\pi$ (n=1,2...) has been a subject of active experimental[1] and theoretical[2] interest. In an early publication[3] discussing the inhibiting influence of level degeneracy on the transparency of large area pulses, it was noted that zero area pulses can propagate with low loss irrespective of the degeneracy of the resonant transition. Such "zero-degree" pulses result if the pulse envelope undergoes a sign change in such a way that the tipping angle,

$$\theta_m(z,t) = \frac{\mu_m}{h} \int_{-\infty}^{t} \mathcal{E}(z,t)dt$$

goes to zero for $t \to \infty$. Here, $\mathcal{E}(z,t)$ is the envelope of the electric field, $\vec{E} = \hat{\varepsilon}\, \mathcal{E}(z,t)\cos(\omega t-kz)$, and μ_m is the dipole matrix element for the transition involving the m^{th} degenerate sublevel. The area $\theta_m(z,\infty) \equiv \theta_m(z)$ measures the degree of excitation of resonant molecules after passage of the pulse.[4] Recent articles have analyzed additional features of zero-degree pulse propagation.[5-7]

We describe here experiments in which zero-degree pulses have been constructed and propagated through a degenerate resonant absorber with dramatically reduced energy loss. We have also observed the evolution of small area pulses into zero-degree pulses due to a resonant absorption and reradiation process,[7,8] discussed in more detail below. The observations are made in the limit of low pulse intensities corresponding to small tipping angles.

A major requirement for low loss propagation is that the pulse be able to coherently excite and de-excite a molecule in a time short compared to the homogeneous transverse relaxation time, T_2.

For a $2n\pi$ pulse ($n > 1$) the pulse energy must be sufficiently large to induce n complete transitions. Because of this, the required pulse energy (proportional to $1/\tau_{pulse}$) may be excessively large in cases where T_2 is very short. On the other hand, a zero-degree pulse need not induce a complete transition; hence it can propagate with low loss even with small energy.

The latter property is of particular interest for propagation of ultrashort pulses through a homogeneously broadened resonant absorber (for example in the atmosphere). If the absorption line is inhomogeneously broadened, small energy zero-degree pulses will still propagate with low loss provided the pulse envelope changes sign before the molecules can dephase due to the spread in their frequency distribution.[9]

The experimental arrangement is shown in Fig. 1(a). A c.w. laser with an internal mirror and diffraction grating line selector is operated on single P or R branch transitions of CO_2 or N_2O in the 10μ region. The linearly polarized output of the laser is passed through a GaAs electro-optic modulator crystal with its $\vec{E}$ field oriented relative to the crystal axes[10] as shown in Fig. 1(b). The crystal is pulsed with a 5 kV/cm square pulse derived from a pressurized spark gap and RG8/U coaxial cable pulse-forming network. The rise and fall time of the pulse is less than 0.3 nsec and the duration can be varied by changing the length of the charging cable [C in Fig. 1(a)]. In the experiments reported here, pulses of 2 or 6 nsec duration were used. The pulse is propagated over the crystal, which is matched to 50Ω by adjusting the capacitance of the crystal holder.

The voltage pulse can be applied to the crystal a second time with the same or opposite polarity by allowing it to reflect from the end of an open or shorted 50Ω cable [R in Fig. 1(a)] which terminates the crystal. Single pulses are obtained by terminating the cable with a 50Ω resistor. For an incident field $E_o \sin(\omega t - kz)$ polarized as shown, the output in the perpendicular polarization, which is selected by analyzer A, is given by $E_o \cos(\omega t - kz) \sin\Gamma$, where $\Gamma = \pi n_o^3 r_{41} V\ell/\lambda d \approx \pi/8$ is the phase advance or retardation (determined by the sign of the electric field strength V/d) along axes a or b [Fig. 1(b)].[11]

The transparency effect was observed in CO_2, using a 1.5 m heated gas cell, as well as in NH_3. The ν_2[asQ(8,7)] transition of $^{14}NH_3$ is coincident to within 10 MHz of the P(13) 10.6μ N_2O laser line and has a Doppler half-width of 42 MHz.[12,13] The NH_3 absorption coefficient of 0.7 cm^{-1}/torr is considerably larger than in CO_2 and hence allowed detailed studies for many absorption lengths. Figure 2 shows a logarithmic plot of experimental data for the transmission of 0.01 w/cm^2 P(13) 10.6μ N_2O laser pulses through a variable pressure[14] 40 cm NH_3 absorption cell [CI in Fig. 1(a)]. Curve A in Fig. 2(a) shows the transmission of zero-degree pulses with two out-of-phase 2 nsec lobes, which are shorter than $T_2^* = 1/2\pi\Delta\nu \approx 4$ nsec (where $\Delta\nu$ is the Doppler half-width of the absorbing transition). The dashed line shows for comparison the transmission of low intensity c.w. radiation as given by $e^{-\alpha L}$, where α is the linear absorption coefficient and L is the length of the sample cell. At low pressures, the number of absorption lengths, αL, is proportional to pressure since the pressure broadening is small compared to the

Doppler width.[15] The effective absorption coefficient for the zero-degree pulses may be obtained from the logarithmic slope of curve A. By comparison with the c.w. absorption (dashed line), we note that at low pressures the absorption coefficient of the 2 nsec zero-degree pulses is smaller by a factor of more than 25 than the value of 0.7 cm^{-1}/torr. (At pressures above 75μ, corresponding to $\alpha L \approx 2$, the slope in curve A increases slightly indicating an increased absorption; this is believed to be due to a small delay between the two pulses which can result in an interference between the second pulse and the molecular reradiation after the first pulse.)

For a short duration pulse of non-zero area, the absorption coefficient is expected to be smaller than α when its duration is less than T_2^*. In this case, the energy absorbed becomes proportional to the pulse duration rather than the inverse linewidth. For a thin sample ($\alpha L < 1$) this reduction is not as great as for the zero-degree pulse of the same duration. For $\alpha L >> 1$, propagation effects cause the pulse area to evolve toward zero (see below). Curve B in Fig. 2(a) shows the transmission of a pulse of non-zero area consisting of two in-phase 2 nsec pulses. The initial absorption obtained from the slope of this curve is less than the c.w. absorption, but larger by a factor of five than that of the zero-degree pulse. At higher pressures, corresponding to several absorption lengths, this curve begins to flatten out and its slope becomes characteristic of that of a zero-degree pulse.

Similar behavior is seen for 6 nsec zero-degree pulses (curve C) and in-phase pulses (curve D), but these exhibit larger absorption

since the pulse is now longer than T_2^*.

We now turn our attention to the evolution of a non-zero area pulse toward zero. Saturation of the medium is negligible in our experiments since for a pulse of duration τ_p=12 nsec (corresponding to two in-phase 6 nsec pulses), and μ=0.2 Debye,[13] the maximum pulse area is less than 2°. For these small angles, the above results can be quantitatively understood[16] in terms of a linearized theory[7] in which the thin sample absorption is proportional to the overlap of the Fourier spectrum of the pulse with the resonance line. A zero-degree pulse has a Fourier spectrum which is zero on resonance. A similar spectrum, and hence absorption, will also result if a non-zero area pulse whose spectral width is broader than the resonance line is allowed to propagate several absorption lengths. A consideration of linear dispersion shows that the phase relationships of the Fourier components are altered in such a way as to yield a zero-degree pulse.[17] For large tipping angles, the nonlinearity invalidates this analytic description, but we know from the area theorem[1-3] that the pulse area will decay toward zero if it is initially less than π.

The evolution of a small area pulse into a low loss zero-degree pulse can alternately be described in the time domain in the following way:[7,8] As the pulse enters the medium, it excites an oscillating macroscopic polarization which for a resonant absorber is phased so as to radiate a field which adds destructively to the incident field. The polarization continues to radiate after the pulse passes and produces a negatively phased lobe on the trailing edge of $\mathcal{E}(z,t)$. For small absorption ($\alpha z \ll 1$, where z is the penetration depth into

the sample), and in the inhomogeneously broadened limit, the coherent "ringing"[8] of the medium lasts for a time comparable to the inverse spectral width of excited atoms, which is given by the longer of the pulse width τ_p or the inverse inhomogeneous width T_2^*. For a homogeneously broadened line, the coherent ringing time will be given by the transverse relaxation time T_2. In either case, the polarization decays before all of the absorbed energy is coherently reradiated. If $\alpha z > 1$, on the other hand, a sufficiently large fraction of the incident pulse has been absorbed and reradiated into the negative lobe to enable this lobe to extract an appreciable fraction of the absorbed energy. This lobe is further amplified as the pulse propagates so that the pulse area approaches zero with little further loss in pulse energy. Significant pulse reshaping, resulting in the development of a pulse with many lobes, is obtained for $\alpha z \gg 1$.[18]

In order to further verify this evolution of small area pulses into zero-degree pulses, a second 40 cm absorption cell (CII) was added in front of the first. With cell CII empty, the transmission of cell CI for 6 nsec and 2 nsec single pulses was measured as a function of pressure and is plotted as the lower curves in Fig. 2(b,c). Cell CII was then filled to pressures corresponding to the absorption marked by the arrows on these curves. The fraction of energy transmitted by CI was again measured as the pressure in CI was varied; the results are plotted on the same graphs. The curve labeled I in each case corresponds to an input pulse which has only partially evolved toward a zero-degree pulse, whereas curve II results from a pulse which has propagated a sufficient number of absorption lengths

to become a good zero-degree pulse. The 6 nsec pulse evolves into one which has an absorption coefficient of only 1/20 that of the c.w.; the 2 nsec into one which has only 1/100. At a pressure of 1 torr, where the c.w. beam is attenuated by $e^{-\alpha L}$ with $\alpha L \approx 20$,[15] 65% of the energy of the 2 nsec pulse which emerges from cell CII is transmitted by cell CI.

It should be noted that at pressures sufficiently high that collision broadening becomes larger than the Doppler width, the dashed curve, which represents the c.w. absorption, becomes parallel to the abscissa. In the pressure region where T_2 becomes shorter than the pulse duration, the absorption for all pulses asymptotically approaches the high pressure limit of the dashed curve. At a fixed pressure, the c.w. absorption maintains a constant logarithmic slope as a function of sample length; the zero area pulse would also exhibit a constant but greatly reduced slope.

The use of short pulses from mode-locked lasers should allow the effects described here to be useful for long distance propagation through absorbers with considerably shorter relaxation times. In the case of atmospheric propagation, for example, typical values for pressure broadening range between 1 and 20 MHz/torr. Pulses 10 to 100 times shorter than those utilized here can be expected to result in low loss propagation.

Other aspects of this work which are still the subject of experimental investigation include the study of these effects in the high intensity limit where the nonlinear effects become important, as well as the off-resonance case, and the observation of the actual pulse envelope distortion.

REFERENCES

1. S. L. McCall and E. L. Hahn, Phys. Rev. Letters 18, 908 (1967); H. M. Gibbs and R. E. Slusher, Phys. Rev. A5, 1634 (1972).

2. S. L. McCall and E. L. Hahn, Phys. Rev. 183, 457 (1969).

3. C. K. Rhodes, A. Szöke and A. Javan, Phys. Rev. Letters 21, 1151 (1968).

4. The effect of level degeneracy on coherent excitation has also been observed in an experiment in which the population change was measured by means of the subsequent fluorescence: see H. P. Grieneisen, N. A. Kurnit and A. Szöke, Optics Communications 3, 259 (1971).

5. F. A. Hopf, C. K. Rhodes, G. L. Lamb, Jr. and M. O. Scully, Phys. Rev. A3, 758 (1971).

6. G. L. Lamb, Jr., Rev. Mod. Phys. 43, 99 (1971). This article also gives a comprehensive review of work in the field of ultrashort pulse propagation.

7. M. D. Crisp, Phys. Rev. A1, 1604 (1970).

8. D. C. Burnham and R. Y. Chiao, Phys. Rev. 188, 667 (1969).

9. Large energy zero-degree pulses of specific shapes, related to 4π pulses, are predicted to propagate with low loss without fulfilling this requirement (see Ref. 5,6). Details of the propagation behavior, such as the pulse reshaping, will be different for these large intensity pulses. Loss of energy from the lower intensity wings of the beam profile may also introduce instabilities.

10. S. Namba, J. Opt. Soc. Am. 51, 76 (1961).

11. The voltage applied to the crystal actually consists of a train

of double pulses separated by the 100 nsec round trip time to the spark gap, since the pulse is again reflected there. Although the effects reported here could be seen with such pulse trains, we present only data taken by using a boxcar integrator with a 30 nsec gate to select the first pair of pulses from the output of the Cu:Ge detector.

12. F. Shimizu, J. Chem. Phys. 52, 3572 (1970); Appl. Phys. Letters 16, 368 (1970).

13. T. Shimizu and T. Oka, Phys. Rev. A2, 1177 (1970).

14. The curves in Fig. 2 were measured as a continuous function of pressure. The points correspond to pressures at which the Pirani pressure gauge was calibrated, by means of a McCleod gauge at pressures above 150 mTorr and by means of the c.w. absorption at lower pressures.

15. The pressure broadening of $\sim$ 25 MHz/torr (see Ref. 12) does not become significant until pressures exceed several hundred mTorr.

16. Cf. Fig. 5 or Ref. 7. A more detailed analysis of these results will be presented elsewhere.

17. It should be noted that regardless of the continuous changes in pulse envelope, the carrier frequency remains unshifted if the laser frequency coincides with the center of a symmetrically shaped absorption line (see Ref. 6,7).

18. This behavior has also been described in terms of the superradiant decay of an N particle system excited by a propagating pulse. See, for example, F. T. Arecchi and E. Courtens, Phys. Rev. A2, 1730 (1970); R. Friedberg and S. R. Hartmann, Physics Letters 37A, 285 (1971).

FIGURE CAPTIONS

Figure 1 (a) Schematic of experimental apparatus. Cell CII is in place only as described in text. The integrated output of the detector (D) is recorded as a function of pressure in cell CI.

(b) Orientation of GaAs modulator.

Figure 2 Transmission of N_2O laser energy through resonant NH_3 absorber as function of pressure. Dashed lines give c.w. absorption.

(a) Transmission through cell CI only for: (A) 2 nsec zero-degree pulses, (B) 2 nsec in-phase pulses, (C) 6 nsec zero-degree pulses, and (D) 6 nsec in-phase pulses.

(b) Transmission of single 6 nsec pulses through cell CI with cell CII filled at fixed pressures to give absorption indicated by arrows on lower curve.

(c) Same as (b), for single 2 nsec pulses.

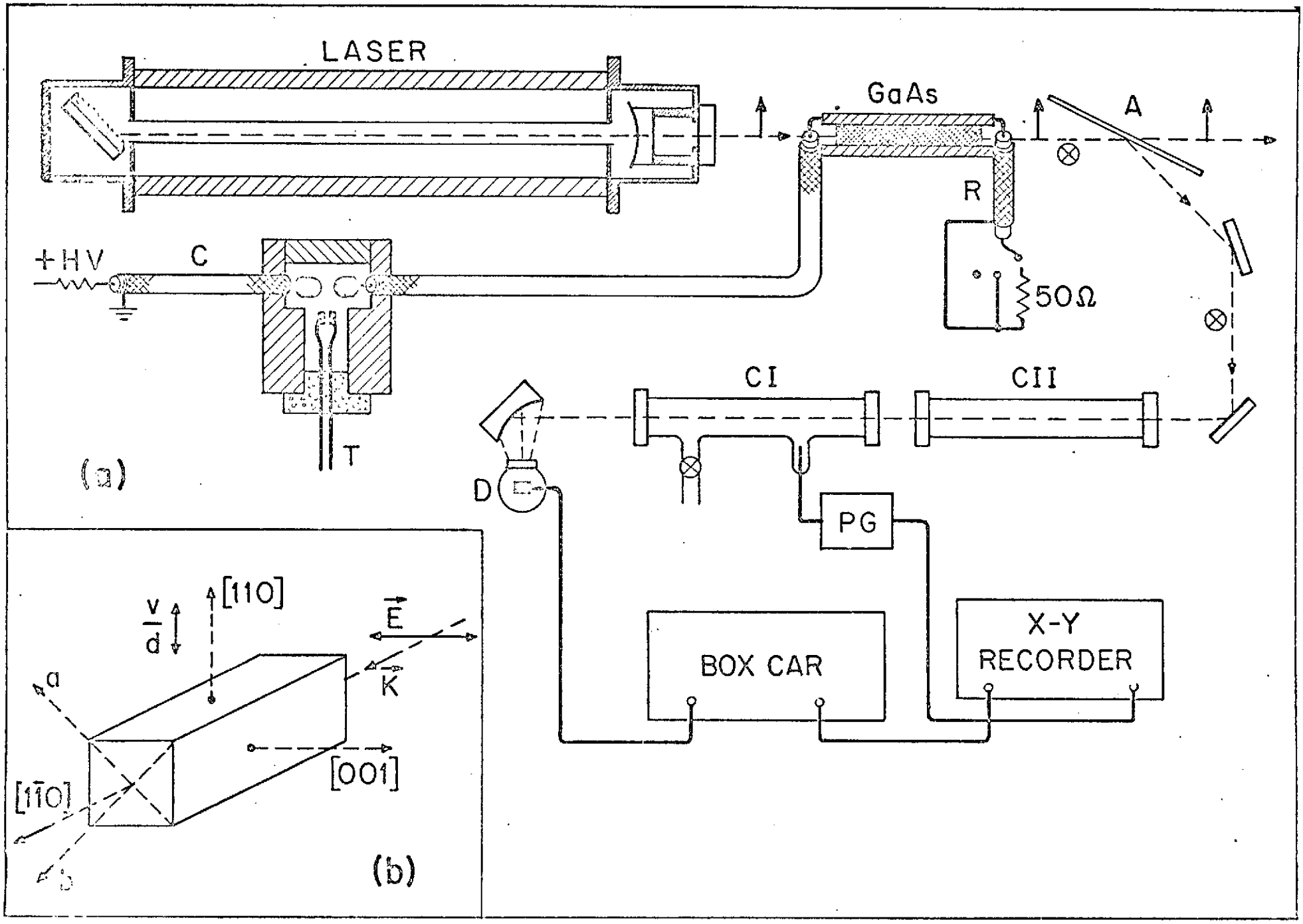
LASER
GaAs
A
R
+HV
C
50Ω
CI
CII
T
(a)
D
PG
BOX CAR
X-Y
RECORDER
v/d
[110]
E
K
a
[001]
[1$\bar{1}$0]
b
(b)

Fig. 1

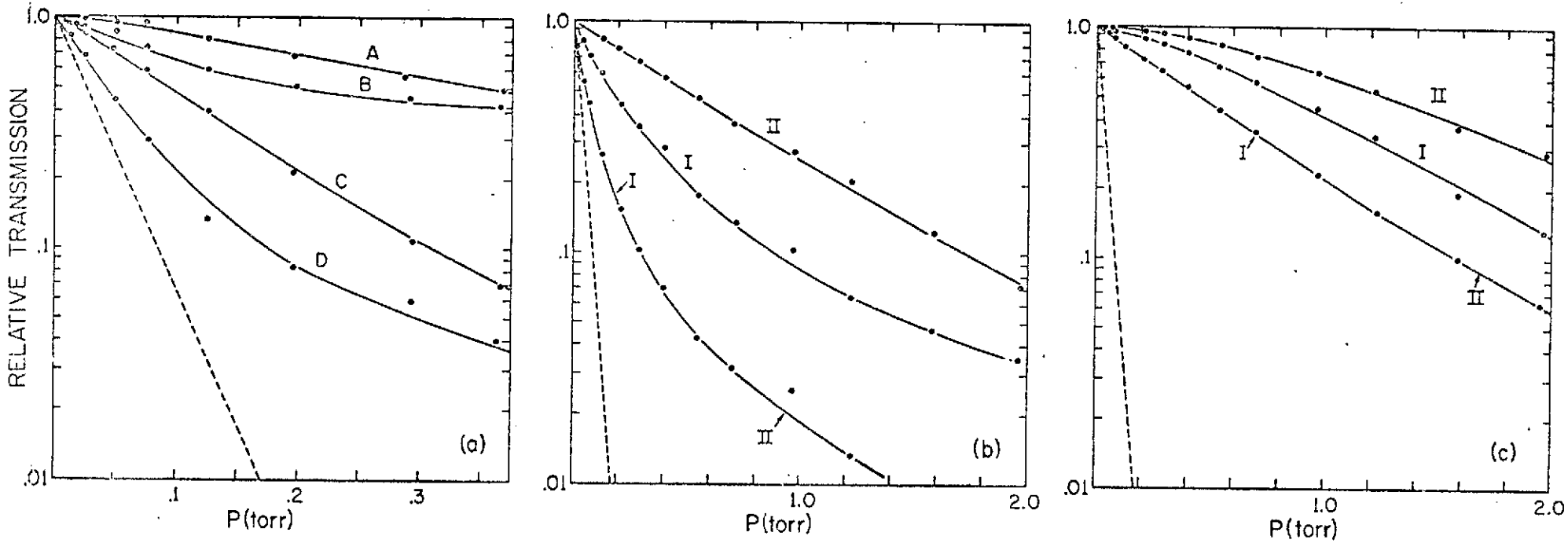
RELATIVE TRANSMISSION
1.0
.1
.01
A
B
C
D
(a)
.1
.2
.3
P(torr)
I
II
(b)
1.0
2.0
P(torr)
(c)

Fig.2

APPENDIX B

OBSERVATION OF DICKE SUPERRADIANCE IN OPTICALLY PUMPED HF GAS*

N. Skribanowitz, I. P. Herman+, J. C. MacGillivray and M. S. Feld

Department of Physics
Massachusetts Institute of Technology
Cambridge, Massachusetts 02139

ABSTRACT

Room temperature HF gas at mTorr pressures, optically pumped to produce a total inversion at a rotational transition in the v=1 vibrational state, is found to emit a superradiant pulse with ringing after a considerable delay ($\sim\mu$sec). A semiclassical analysis shows that for a high gain system the pulse evolution is determined by a single parameter, τ_R, and that inhomogeneous broadening is unimportant. Close agreement between theory and experiment is obtained.

* Work supported in part by the National Science Foundation

+ Hertz Foundation predoctoral fellow

This paper[1] reports the first detailed study of Dicke superradiance[2,3] in the optical region.[4] In the experiments a long sample cell of low pressure (∿mTorr) HF gas is pumped by an intense short pulse from an HF laser operating on an R or P branch transition to the vibrational ground state (λ∿2.5μm). This produces a nearly complete population inversion between two adjacent rotational levels in the v=1 state, corresponding to transitions in the 50 to 250 μm range.[5] After a considerable delay (∿μsec) a burst of radiation appears at the rotational transition (Fig. 1). The formation, delay, and ringing of this radiation pulse are of major interest in this study.

As pointed out by Dicke,[2] a totally inverted two level system can give rise to a superradiant pulse. In the Bloch formalism the initial state corresponds to a vector pointing straight up, in analogy to the unstable equilibrium position of a rigid pendulum standing exactly on end. Though this state cannot radiate classically, a macroscopic polarization develops in the medium, triggered by incoherent spontaneous emission and background thermal radiation, the "perturbing field." In the absence of collisions the system gradually evolves into a superposition of superradiant states, corresponding to the Bloch vector pointing sideways, at which time the radiation pulse is emitted. This pulse can be considerably delayed with respect to the sudden switching on of the population inversion. In order to produce long delays it is necessary to excite the system without leaving a macroscopic polarization in the medium. This condition is difficult to achieve by coherent excitation of a two-level

system but it is easily fulfilled by optically pumping the system via a coupled transition.

In numerous treatments of superradiance the radiation field is quantized and the atomic system is described in terms of collective Dicke states.[6] As pointed out by Arecchi et al,[7] these atomic states can be used to construct a new set of states, called Bloch states, which have similar properties to Dicke states, but may be treated semiclassically by means of the coupled Maxwell-Schrödinger equations.[8] The semiclassical approach is not justified during the initial stage of pulse evolution, where stimulated emission is not yet dominant.[9] However, as seen below, the form of the initial fluctuations is unimportant. Adopting this approach, we use the coupled Maxwell-Schrödinger equations,[10] including homogeneous and inhomogeneous broadening, linear loss (diffraction), and level degeneracy, to treat a weak perturbing field, simulating spontaneous emission and black body radiation, incident on a rod-shaped medium which is inverted at t=0. An important result of the analysis[11] is that the pulse evolution can be described simply in terms of only two parameters, τ_R, a characteristic time for the radiation damping of the collective system, and $\alpha\ell$, the linear field gain:

$$\tau_R = 8\pi(N\lambda^2\ell)^{-1}T \quad , \tag{1}$$

and

$$\alpha\ell = T_2^*/\tau_R \quad . \tag{2}$$

Where λ is the wavelength, N the net population inversion density, T the radiation lifetime of an isolated atom, T_2^* the dephasing time of the rotational transition,[12] and ℓ is the length of the sample cell. In particular:

1. The area of the output pulse is completely determined by the gain, $\alpha\ell$, and the area of the perturbing field over the first few τ_R, $\theta(0)$, in accordance with the area theorem of McCall and Hahn,[13] valid for an inhomogeneously-broadened non-degenerate[14] system. Since in our case $\theta(0) \sim 10^{-8}$, gains in excess of 20 are needed for appreciable pulse build-up. Such gains are available in HF at mTorr pressures.[5]

2. For a given value of $\alpha\ell >> 1$, the time scale of the pulse evolution (i.e. delays, pulse shapes) is completely determined by τ_R.

3. For fixed $\alpha\ell$ and τ_R, inhomogeneous broadening, level degeneracy[14] and a reasonable amount of linear loss change the results in minor ways.[15]

4. The pulse delay, τ_D, depends linearly on τ_R,[11]

$$\tau_D = [\ell n\theta(0)]^2 \tau_R/4 \quad , \qquad (3)$$

and this is confirmed in the experiments.

The change in delay caused by perturbing fields of different sizes is related to the problem of gently tipping over a rigid pendulum balanced on its end: The stronger the initial tap, the faster the pendulum will fall. Also, as with a pendulum, only the first few degrees of tipping progress slowly. Once the Bloch vector has tipped

appreciably, it falls the rest of the way rapidly (in a few τ_R).

Numerical calculations, described below, confirm these predictions and also lead to the following conclusions:

¶ The effects of relaxation are unimportant as long as the homogeneous relaxation time, T_2, exceeds the pulse delay. (At the mTorr pressures of the experiments T_2, determined by collisions, is always much longer than the delays.)

¶ The effectiveness of the perturbing field is limited to the first few τ_R's. Furthermore, the system behavior is insensitive to the exact form of the initial perturbation. Delta function, step function, Gaussian pulses and pulse trains of intensity consistent with the magnitude of the background radiation field all give output pulses of the same shape and delay. Furthermore, the presence of random jumps in the phase of the input field to simulate spontaneous emission does not significantly affect the output pulses. This justifies our approach.

¶ The output pulses are insensitive to the specific time dependence of the population excitation.

The experimental arrangement consisted of an HF pump laser, a sample cell and the detection system. The pump laser, a helical pin laser described previously[5] produced $R_1(J)$ and $P_1(J)$ pulses of 200-400 nsec duration and peak powers of a few kW/cm^2. The stainless steel sample cells ranged in length from 30 to 100 cm, with inner diameters between 12 and 28 mm. They had silicon Brewster windows coated on the inside with a thin layer of Halocarbon stopcock grease to prevent corrosion. The HF gas was purified by freezing and dis-

tillation. The pressure in the sample cell was estimated from the linear attenuation of the pump laser output. To observe the superradiant pulses a helium cooled In-Ge detector was used, followed by a fast pre-amplifier and a pulse amplifier. The overall rise time of the system was below 10 nsec, giving ample resolution of the pulse shapes.

The HF lines studied were the J+1→J rotational transitions in the v=1 band, with J ranging from 0 to 4, corresponding to the wavelengths 252, 126, 84, 63 and 50 μm. All of these lines have been obtained previously by optical pumping at much higher pressures.[5] The sample cell was optically pumped in a single pass, leading to superradiant output pulses with peak intensities estimated to be in the 100 $\mu W/cm^2$ range and widths in the range of 50 to several hundred nsec, depending on the gas pressure and pump laser power. This corresponds to pulse areas of order unity. Care was taken to unsure that no far-infrared radiation from the pump laser entered the sample cell.

Since both pump and rotational transitions are Doppler-broadened, the gain is independent of the pump laser intensity provided the pump transition is saturated.[11] Therefore, in our experiments the gain is selected by fixing the sample cell pressure, and τ_R may then be adjusted by varying the pump intensity.

Figures 1 and 2 show oscilloscope traces of superradiant pulses under various experimental conditions. At pressures below 5 mTorr the pulses were delayed by 500 to 2000 nsec past the beginning of the pump pulse. Decreasing the pressure increased the delays, broadened the pulses and decreased their magnitude, in agreement with theoretical expectations [Fig. 2(a,b)].[16] Two microsecond delays, the

longest observed, occurred at pressures below 1 mTorr. (At high pressures, i.e. above 10 mTorr, the pulses were single spikes 40 nsec in width and occurred during the pump pulse.) Furthermore, decreasing the pump power increased the pulse delay and width and decreased its amplitude [Fig. 2(c,d)], again in agreement with theory. The pulses often exhibited ringing with as many as four lobes (Fig. 1). Similar pulses were also seen in the backward direction, i.e. propagating antiparallel to the traveling-wave pump radiation.

To compare experiment with theory we have integrated the coupled Maxwell-Schrödinger equations given in Eq. (208) of Icsevgi and Lamb,[10] modified to include level degeneracy, as is necessary in treating molecular systems. All parameters are expressed in terms of the three experimental variables, the pump field intensity, I, the sample cell pressure, p, and the incremental loss, κ. These values, estimated from the experimental conditions, are given in the figure captions. In addition, it is necessary to specify the pump transition used. All the calculations assume a collision time of T_2=7 μsec at 1 mTorr. An input field envelope of constant amplitude is used. Its magnitude, E_0, estimated from black body radiation and spontaneous emission intensity ($\sim 10^{-14}$ W/cm^2), depends on I and p and ranges from 10 to 50 sec^{-1}, in units of $\mu E_0/\hbar$. The rotational levels are inverted over a period of ~100 nsec to take account of the pump pulse duration. As can be seen in the figures good agreement is obtained throughout.

The presence of feedback in our high gain system drastically

shortens the pulse delays, as was verified by intentionally introducing feedback. Estimates show that for gains typical of our experiments feedback of the order of 10^{-4} to 10^{-5} is permissible. Scattering off the cell windows into the gain volume is estimated to be at least a factor of ten smaller than this. Other sources of feedback are even less important. The absence of regeneration was verified by placing a second HF cell after the first one, with a common window between them oriented at Brewster's angle. Both were excited by the same pump laser beam. The first cell was filled to produce long delays, and the second cell was filled to produce large signals and short delays. The pulses of the first cell were observed through a side window positioned to intercept the weak reflection off the common window. The delay and appearance of these pulses was not affected by the presence of the second cell, demonstrating the absence of significant amounts of feedback.

In conclusion, we would like to stress that a superradiant pulse can evolve in an inhomogeneously broadened extended sample. This is because in an amplifier, in contrast to an absorber, dephasing is couteracted by high gain, giving rise to an effective dephasing time[11] $\alpha \ell T_2^*$. This time is always considerably longer than the pulse evolution time τ_D. Furthermore, the bandwidth of the initial perturbation is larger than $1/T_2^*$.[11] Therefore, the time scale of the pulse evolution (determined by τ_R) depends on the <u>total number</u> of excited molecules, irrespective of the extent of inhomogeneous broadening. These points are verified in the experiments.

We are grateful to Ali Javán, Norman Kurnit and Abraham Szöke for helpful discussions, and to Barry Feldman for providing an initial version of the computer program.

REFERENCES

1. An initial account of this work was given by M. S. Feld at the P. N. Lebedev Physical Institute, Academy of Science, U.S.S.R. on September 22, 1972.

2. R. H. Dicke, Phys. Rev. 93, 99 (1954).

3. R. H. Dicke, in Proceedings of the Third Quantum Electronics Conference, Paris 1963, ed. by Grivet and Bloembergen (Columbia Univ. Press, New York, 1964). p. 35.

4. A number of coherent optical effects closely related to the concepts used to treat superradiance have been observed. These are reviewed by E. Courtens in Laser Handbook, ed. by F. T. Arecchi (North Holland Publishing Co., Amsterdam, 1972) p. 493.

5. N. Skribanowitz, I. P. Herman, R. M. Osgood, Jr., M. S. Feld and A. Javan, Appl. Phys. Letters 20, 428 (1972).

6. See R. Bonifacio, P. Schwendimann and F. Haake, Phys. Rev. A4, 302 (1971), and references contained therein.

7. F. T. Arecchi, E. Courtens, R. Gilmore and H. Thomas, Fundamental and Applied Laser Physics: Proceedings of the Esfahan Symposium, ed. by M. S. Feld, N. A. Kurnit and A. Javan (John Wiley and Sons, New York, 1973).

8. F. T. Arecchi and E. Courtens [Phys. Rev. A2, 1730 (1970)] have also pointed out that superradiance may be treated semiclassically.

9. This stage extends over a period $\sim\tau_R$, as can be seen by calculating the time necessary for the first photon to be emitted into the diffraction mode determined by the sample geometry. Also note that the pulses evolve over a period $\sim 100\ \tau_R$ [cf. Eq. (3)].

10. See, for example, A. Icsevgi and W. E. Lamb, Jr., Phys. Rev. 185, 517 (1969).

11. I. P. Herman, J. C. MacGillivray, N. Skribanowitz and M. S. Feld, Phys. Rev., to be published.

12. The inhomogeneously-broadened line width of the rotational transition is $\Delta=1/T_2^*$. For a Doppler-broadened transition $\Delta=ku/\pi^{1/2}$, where ku is the half width of the Doppler profile at the 1/e point in units of circular frequency.

13. S. L. McCall and E. L. Hahn, Phys. Rev. 183, 457 (1969).

14. The consideration of Rhodes, Szöke and Javan [Phys. Rev. Letters 21, 1151 (1968)] applied to an amplifier show that level degeneracy does not inhibit pulse evolution and that pulses of increasing energy but stable area near π can evolve.

15. These approximations lead to an analysis similar to that of D. C. Burnham and R. Y. Chiao [Phys. Rev. 188, 667 (1969)] applied to an amplifier rather than to an absorber.

16. At high pressures the signal size also decreased with decreasing pump intensity. At intermediate pressures ($\sim$10 mTorr), however, decreasing the pump power actually increased the signal amplitude.

FIGURE CAPTIONS

Figure 1. Oscilloscope trace of superradiant pulse at 84 μm (J=3→2), pumped by the $R_1(2)$ laser line, and theoretical fit. The parameters are I=1kW/cm^2, p=1.3 mTorr and $\kappa\ell$=2.5 for ℓ=100 cm. The small peak on the scope trace at τ=0 is the 3μ pump pulse, highly attenuated.

Figure 2. Oscilloscope traces of superradiant pulses and computer fits. a) J=3→2 transition at 84 μm pumped by $P_1(4)$ laser line. I=2.2 kW/cm^2, p=4.5 mTorr, $\kappa\ell$=2.5 (ℓ=100 cm). b) Same as (a) but p=2.1 mTorr. Note increased delay and broadening of pulse. c) Same transition as in (a), but pumped by $R_1(2)$ laser line. I=1.7 kW/cm^2, p=1.2 mTorr, $\kappa\ell$=3.5 (ℓ=100 cm). d) Same as (c) except I=0.95 kW/cm^2. The same intensity scale is used in fitting curves (a) and (b), and (c) and (d). Note the reproducibility of the oscilloscope traces in double exposure.

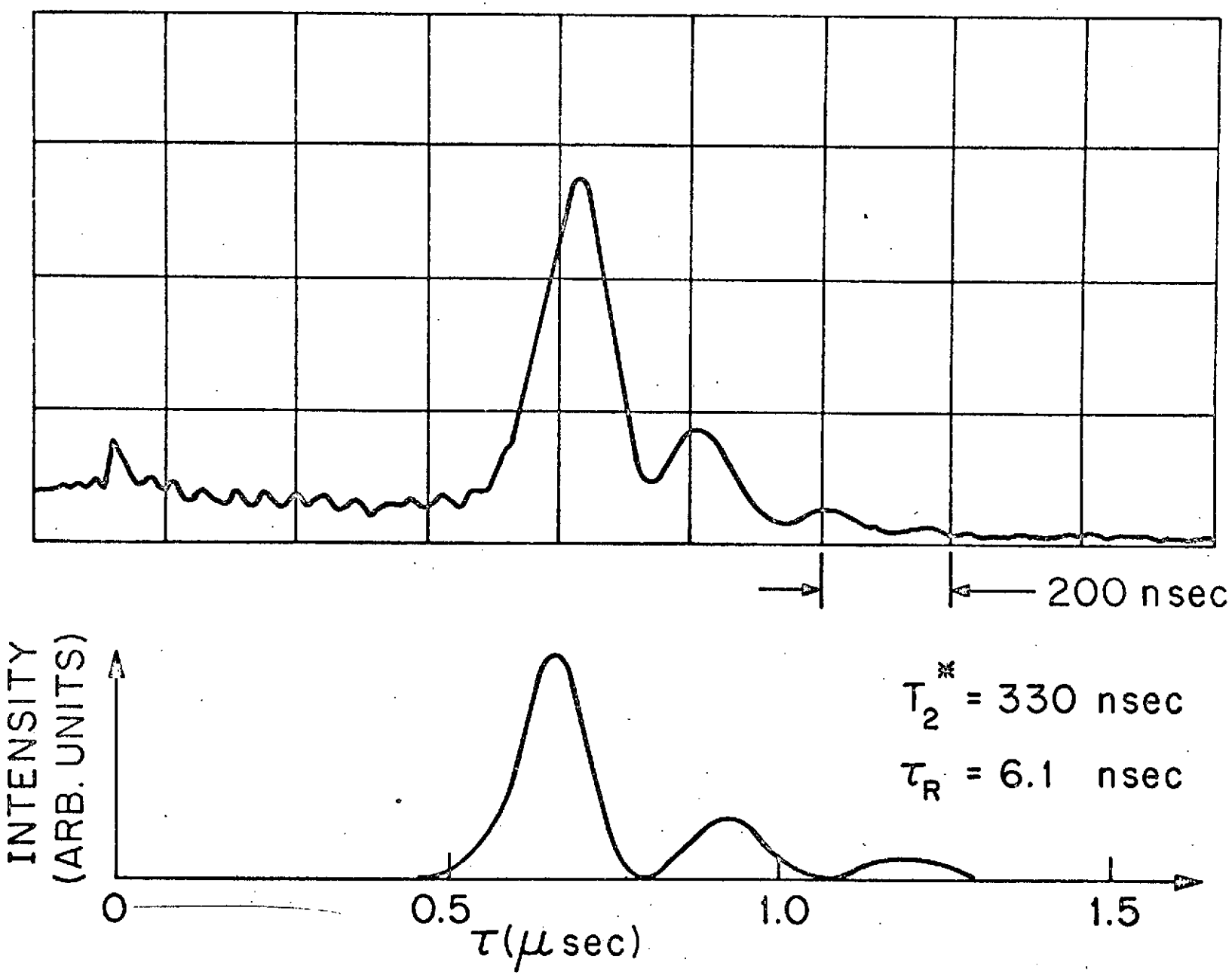
200 nsec
INTENSITY
(ARB. UNITS)
$T_2^* = 330$ nsec
$\tau_R = 6.1$ nsec
0
0.5
1.0
1.5
$\tau(\mu sec)$

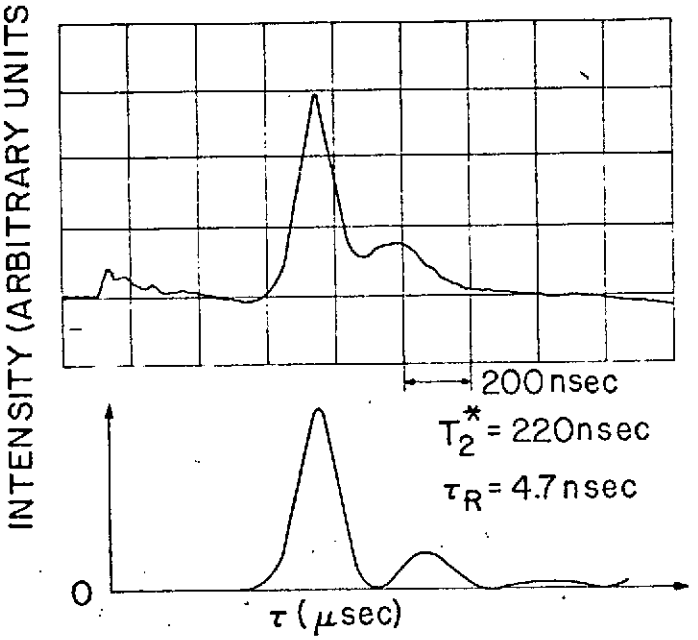
INTENSITY (ARBITRARY UNITS)
200 nsec
T_2^* = 220 nsec
τ_R = 4.7 nsec
0
τ (μsec)

(a)

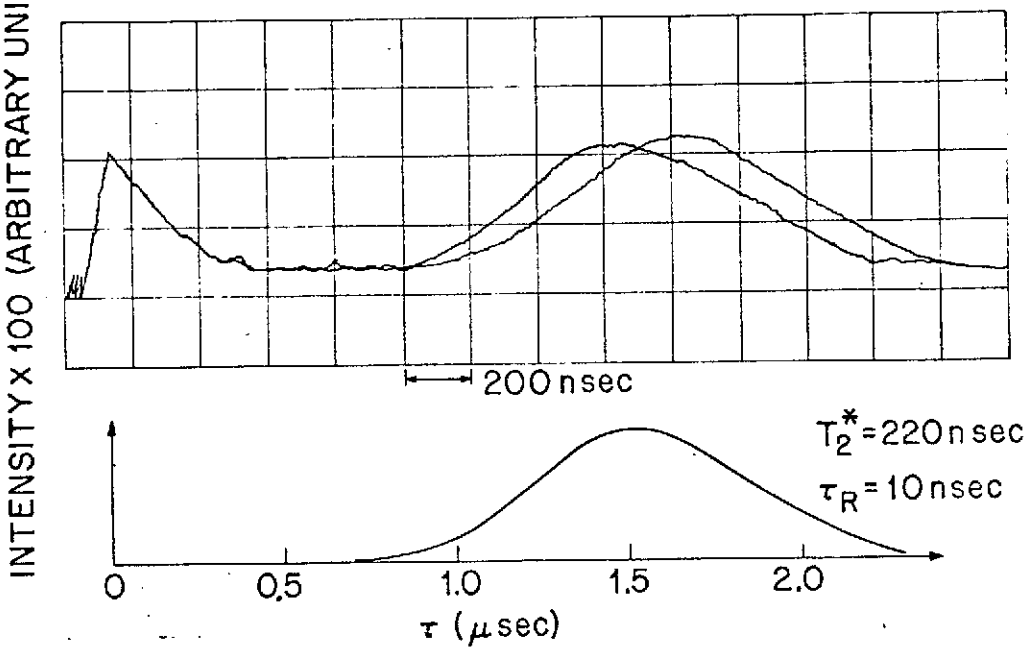
INTENSITY X 100 (ARBITRARY UNITS)
200 nsec
T_2^* = 220 nsec
τ_R = 10 nsec
0
0.5
1.0
1.5
2.0
τ (μsec)

(b)

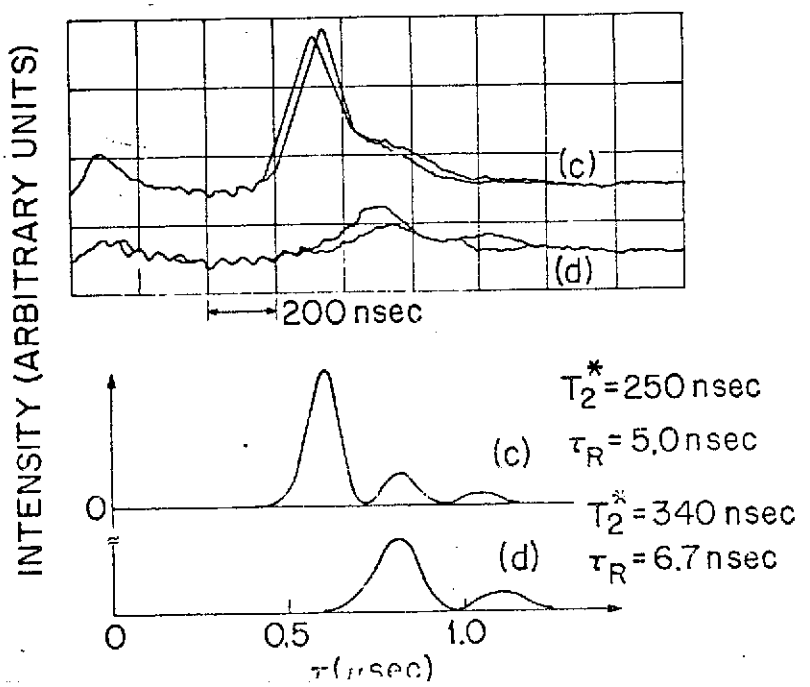
INTENSITY (ARBITRARY UNITS)
(c)
(d)
200 nsec
T_2^* = 250 nsec
(c) τ_R = 5.0 nsec
0
T_2^* = 340 nsec
(d) τ_R = 6.7 nsec
0
0.5
1.0
τ (μsec)

APPENDIX C

ANISOTROPIC ULTRA-HIGH GAIN EMISSION OBSERVED IN ROTATIONAL TRANSITIONS IN OPTICALLY PUMPED HF GAS

N. Skribanowitz, I. P. Herman, R. M. Osgood, Jr., M. S. Feld and A. Javan

Department of Physics
Massachusetts Institute of Technology
Cambridge, Massachusetts 02139

ABSTRACT

Gain and laser oscillations are obtained on rotational transitions of the first excited vibrational state of HF gas at room temperature, resonantly pumped by the 2.7μ lines of a pulsed HF laser. Pumping the P-branch transitions connecting the ground and first excited vibrational states produces gain at the coupled rotational transitions at 36, 42, 51, 84 and 126 μ. The gain exhibits directional properties characteristic of a unidirectional amplifier predicted by a recent theory. The incremental gains of these lines is very large, in excess of 1 per cm, and the lines oscillate easily without mirrors ("super-radiance").

This letter reports observation of gain and laser oscillations in rotational transitions of the first excited vibrational state of pure HF gas at room temperature, pumped by the 2.7μ lines of a pulsed HF laser. The gain shows anisotropy characteristic of a unidirectional amplifier predicted by a recent theory[1]. The gain in these lines is enormous and they oscillate easily without mirrors ("superradiance").

Laser oscillations of rotational lines in excited vibrational molecular states have been produced in other gases by optical pumping from the ground vibrational state[2]. The present study also makes use of optical pumping, but the emitted radiation shows unidirectional features not obtained before. These features are caused by the traveling wave pumping of Doppler-broadened transitions. The ultra-high gain of these lines in HF facilitates the observation of the effects.

The HF sample cell was pumped in a single pass by one of the 2.7μ $P_1(J)$ lines of an HF laser, where the notation $P_1(J)$ indicates P-branch transitions connecting the ground and first vibrational states of HF: $(v,J) = (1, J-1) \rightarrow (0,J)$. Gain was observed at the coupled rotational transition $(1,J-1) \rightarrow (1,J-2)$ in the excited vibrational state [Fig. 1(a)]. These transitions fall in the far-infrared (36 - 126μ).

The pump laser was a helical transverse discharge HF "pin" laser using a mixture of SF_6 and H_2[3,4]. The laser cavity consisted of a 2μ diffraction grating and a gold-coated sapphire flat. Individual $P_1(J)$ laser lines could be selected by tuning the grating. Power was coupled out through a 4.5 mm diameter hole in the gold-

coating of the flat. The output pulses typically had a length of one microsecond and a peak power of 3-4 kW as measured with an Epley thermopile.

The absorption cell and the HF gas handling system were made of Monel metal. The cell was 12 cm long with an inner diameter of 12 mm, and had silicon Brewster windows. The windows were coated with a thin layer of Halocarbon standard stopcock grease to prevent degradation due to HF corrosion. Each window had a transmission of approximately 65% in the wavelength range of interest.

The HF gas was purified several times by freezing it at liquid nitrogen temperature and then pumping on it with a diffusion pump. To eliminate water vapor contamination the HF was kept in a Monel cold trap maintained at -30°C to -40°C by an ethyl alcohol - water slush. The absorption cell was filled with HF to an appropriate pressure and then isolated from the rest of the system. The pressure was ascertained from the linear attenuation of the pump beam, suitably attenuated using filters. Pressures ranged from 50 mTorr to 6 Torr depending upon the line studied.

The far-infrared lines were detected with a helium cooled In-Ge detector. The pump lines were filtered out using a thin sheet of black polyethylene. A monochromator with a 135μ grating was used to determine the wavelengths of the rotational lines.

The observed rotational lines are given in Table I. None of these lines have been observed before[5]. All of the lines were strong and easily detectable except for the 63.4μ line, which is strongly absorbed by atmospheric water vapor. The lines all oscillated without external mirrors[6]. This implies very high gains

since the absorption cell is only 12 cm long. The output powers were estimated from the detector calibration to be in the mW range.

The intensity of the lines depends strongly on pressure. This is due to a trade-off between the number of atoms available and the extent of saturation. At low pressures the saturation is high but the number of atoms is low, whereas at high pressures the reverse is true. This implies an optimum pressure for a given pump power. For all of the observed lines the optimum pressure was found to be such that approximately 50 - 75% of the pump beam was absorbed[8]. These pressures ranged from approximately 50 mTorr for the $P_1(3)$ and $P_1(4)$ pump lines to about 6 Torr for the $P_1(8)$ line. This large variation is due to the fact that the absorption coefficients of the pump transitions change by two orders of magnitude going from $P_1(3)$ to $P_1(8)$.

The unidirectional theory[1] predicts larger gain in the forward direction (i.e. parallel to the propagation direction of the 2.7μ pump field) than in the backward direction. The gain anisotropy was first studied by comparing the intensities of the radiation emitted by the sample cell in the forward and backward directions under high-gain conditions where regenerative feedback (mirrors) was unnecessary. The intensities in the forward direction were found to be 5 to 10 times larger than those in the backward direction[9].

To further investigate the gain asymmetry we placed the sample cell in a ring cavity[10] consisting of two gold-coated mirrors of radii of curvature 8 m and 1.5 m, respectively, and a BaF_2, KBr or NaCl flat, depending on the far-infrared line studied (Fig. 2).

The pump power was coupled in through the flat, which is transparent in the near-infrared and highly reflective and also opaque (Reststrahlen bands) in the far-infrared, thus serving to decouple the gain cell from the optics associated with the pump laser. The cavity was about 1 meter long. About 1% of the far-infrared power was coupled out by means of a saran-wrap beam splitter. The forward and backward intensities were studied separately. In each case the cavity length was tuned to give maximum output power. The maximum power emitted in the forward direction was found to be 40 to 400 times larger than the maximum backward power. In the ring configuration the intensity was very stable, whereas in an open system the intensity fluctuated strongly from one pulse to the next.

In another test the pump laser intensity was attenuated by a factor of 15 (peak power $\sim$200 watts) using absorbing glass plates. Under these conditions the ring cavity oscillated only in a direction parallel to the pump beam. No signal could be detected traveling in the opposite direction. However, the forward signal was close to threshold and not very stable. This is consistent with the theoretical expectations discussed below.

A brief account of the unidirectional effect may be useful. A normally absorbing transition can be brought into the amplifying phase by resonantly pumping a coupled absorbing transition with an intense monochromatic field [Fig. 1(a)]. If both transitions are Doppler-broadened the gain occurs over a narrow frequency interval determined by the homogeneously broadened linewidth (e.g. due to collisions). It was pointed out in Ref. 1 that if the pump field

is in the form of a traveling wave, gain at the coupled transition for waves traveling in the forward direction occurs at one frequency, whereas the gain in the backward direction appears at a different frequency, symmetrically located on the opposite side of the Doppler profile [Fig. 1(b)]. The frequency separation between forward and backward gain regions is proportional to the detuning of the pump field from the line center of the pump transition, and if the pump frequency is tuned close to line center, forward and backward gain regions overlap. An important feature of this effect (independent of whether or not the gain regions overlap) is that the gain in the forward direction is larger than that in the backward direction. This asymmetry arises from the well known width difference between forward and backward change signals observed in laser-induced line-narrowing experiments[11,12]. The difference in gain can be very large. This explanation accounts for the forward-backward intensity asymmetry observed in the experiments described above.

In applying these considerations to HF an important fact must be noted. Goldhar, et al[3] have found that a transversely excited HF laser always oscillates within a range of less than 70 MHz about line center. It is therefore expected that in our experiments the forward and backward gain regions should overlap. To verify this the single pass output, either forward or backward, was reflected back through the cell by means of a BaF_2 flat placed normal to the pump beam. (BaF_2 was used to prevent the pump laser beam from being reflected back and, hence, producing a standing wave, which would eliminate unidirectional features.) Under these conditions the output intensity was considerably larger and much more stable than in the single pass configuration. In fact, the double pass

arrangement enabled the observation of signals which could not be detected otherwise. The fact that the output intensities in the single pass configuration fluctuated considerably from pulse to pulse, even though the output from the pump laser was fairly stable, indicates spurious feedback due, for example, to back scattering from dust particles or windows or backward Rayleigh scattering in the air[6,7].

A rough estimate of the gains of these lines can be made from the observation that in the ring cavity configuration, where a gain of about 1 per pass is needed to overcome losses, the threshold power is approximately 200 W. Therefore, at normal operating powers (3 - 4 kW) the gain coefficient should be 15 to 20 times larger, leading to an incremental gain of over 1/cm. The theoretically predicted values are consistent with these estimates.

Only qualitative agreement between theory[1,13] and experiment can be expected at present since the theory assumes a monochromatic pump field interacting with fully Doppler-broadened transitions. The frequency purity of pulsed HF "pin" lasers is notoriously poor[3]. Frequency chirping and mode jumping may occur during a pulse due, in part, to changes in the refractive index of the plasma during the discharge pulse. Furthermore, the unidirectional effect is expected to decrease for the shorter wavelength lines (36 - 50μ), which oscillate best at sample cell pressures where the collision broadened width is beginning to become comparable to the Doppler width. However, the longer wavelength transitions are fully Doppler-broadened at optimum pressures.

Laser oscillation on one rotational transition can, in principle,

produce cascade oscillations on other transitions lower down in the rotational ladder, especially if the laser oscillation saturates the rotational transition. However, our far-infrared lines are too weak to saturate their transitions, and cascading has not been observed.

In our studies $P_1(J)$ lines were used to pump the excited state rotational transitions. The $R_1(J)$ lines near 2.4μ [$(v,J) = (1,J+1) \rightarrow (0,J)$] are also produced by our HF laser, but at powers about 10 times smaller. In view of the low thresholds observed, the $R_1(J)$ lines can probably also be used as pump fields. Pumping of the $R_1(J)$ transitions also opens the possibility of observing unidirectional emission of $P_1(J)$ lines near 2.7μ.

It is interesting to note that for amplification observed at wavelengths longer than 50μ, kT at room temperature exceeds the quantum energy hν, hence the output signals are triggered by thermal radiation. An attempt was made to observe this effect by placing a globar heat source at the amplifier input. Unfortunately, spurious feedback as described earlier caused considerable fluctuations in the output signal, thus masking the effect. Further studies are currently under way.

We would like to thank Professor E. V. George for giving us the design for the helical HF pin laser, and Thomas C. Rounds, Richard Mendelsohn and Charles J. Wurrey for measuring the far-infrared transmission of various materials and for supplying us

with a black polyethylene filter. Special thanks go to L. W. Ryan, Jr. and to A. Erikson for valuable technical assistance and advice.

REFERENCES

1. N. Skribanowitz, M. S. Feld, R. E. Francke, M. J. Kelly and A. Javan, Appl. Phys. Letters 19, 161 (1971).

2. See, for example, T. Y. Chang, T. J. Bridges and E. G. Burkhardt, Appl. Phys. Letters 17, 249 (1970); 17, 357 (1970); and T. Shimizu and T. Oka, Phys. Rev. 2A, 1177 (1970).

3. J. Goldhar, R. M. Osgood, Jr., and A. Javan, Appl. Phys. Letters 18, 167 (1971).

4. D. R. Wood, E. G. Burkhardt, M. A. Pollack and T. J. Bridges, Appl. Phys. Letters 18, 112 (1971).

5. T. F. Deutch [Appl. Phys. Letters 11, 18 (1967)] has observed laser oscillations arising from rotational transitions in the same band using a pulsed discharge in a 2 m cavity. His lines originate from levels having much higher J values.

6. There are indications that in this configuration non-resonant feedback due to scattering, e.g. from the cell windows or from air, influences the observed output, hence, the assumption of single pass gain may not be valid. For a discussion of non-resonant feedback see Ref. 7.

7. R. V. Ambartsumyan, N. G. Basov, P. G. Kryukov and V. S. Letokhov, Soviet Phys. JETP 24, 481 (1967) [J. Exptl. Theoret. Phys. (U.S.S.R.) 51, 724 (1966)]; R. V. Ambartsumyan, S. P. Bazhulin, N. G. Basov and V. S. Letokhov, Soviet Phys. JETP 31, 234 (1970) [J. Exptl. Theoret. Phys. (U.S.S.R.) 58, 441 (1970)].

8. Note that this figure refers to saturated absorption, as opposed to the linear absorption used to measure the pressure.

9. It might be argued that this asymmetry is due in part to the fact that the gain at the entrance of the cell is larger than at the exit, since the pump beam is attenuated by about 50% in

traversing the cell. But note that spatial variations in gain can cause a forward - backward asymmetry only if saturation occurs. This is not the case for our system, as can be ascertained from the observed output powers.

10. Note that a ring cavity decouples forward and backward traveling waves and, at the same time, eliminates the question of spatial gain variations since the cell is traversed many times by the far-infrared radiation.

11. M. S. Feld and A. Javan, Phys. Rev. 177, 540 (1969).

12. When the pump transition is highly saturated, the gain profile in the forward direction shows additional structure. These effects are discussed in Ref. 13.

13. B. J. Feldman and M. S. Feld, Phys. Rev. (Feb., 1972), and N. Skribanowitz, M. J. Kelly and M. S. Feld, J. Mol. Spectroscopy, to be published.

TABLE I

Pump Transition		Coupled Transition (v=1 excited state)	
Designation*	Wavelength	$J_{Upper} \rightarrow J_{Lower}$	Wavelength
$P_1(3)$	2.608μ	2 → 1	126.5μ
$P_1(4)$	2.639μ	3 → 2	84.4μ
$P_1(5)$	2.672μ	4 → 3	63.4μ
$P_1(6)$	2.707μ	5 → 4	50.8μ
$P_1(7)$	2.744μ	6 → 5	42.4μ
$P_1(8)$	2.782μ	7 → 6	36.5μ

*$P_1(J)$ signifies the (v=1,J-1) → (v=0,J) transition.

FIGURE CAPTIONS

Fig. 1 a) Energy level diagram. The level (v,J) has vibrational quantum number v and rotational angular momentum quantum number J.

b) Gain profile of an HF rotational transition, resonantly pumped at a coupled vibrational transition. The gain in the forward and backward directions occurs over narrow frequency intervals symmetrically located about line center. Note that the gain in the forward direction is larger than that in the backward direction.

Fig. 2 Ring laser cavity configuration. Forward (backward) far-infrared output power is coupled out of the cavity when the beam splitter is in position a(b).

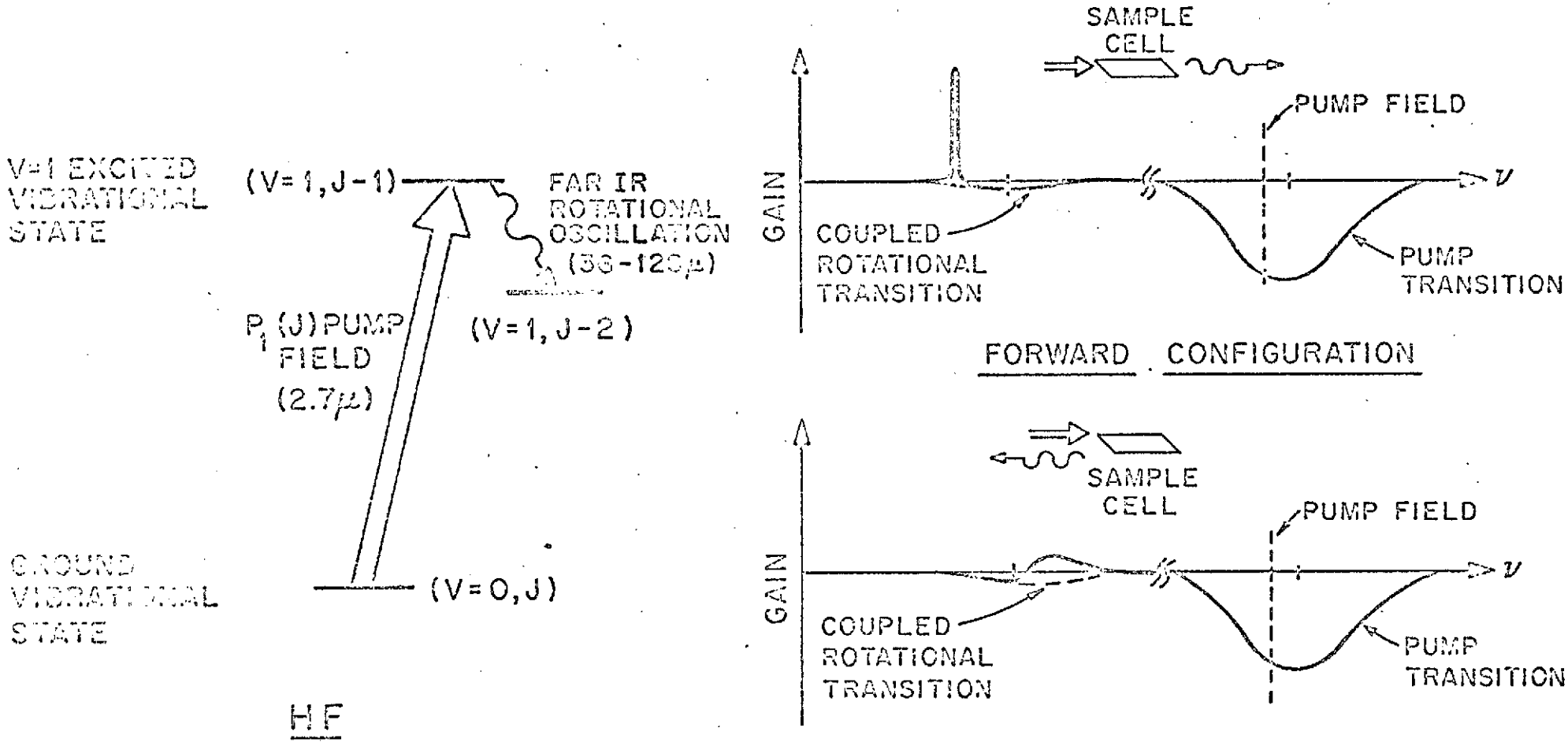
V=1 EXCITED VIBRATIONAL STATE
(V=1, J-1)
FAR IR ROTATIONAL OSCILLATION (50-120μ)
P1 (J) PUMP FIELD (2.7μ)
(V=1, J-2)
GROUND VIBRATIONAL STATE
(V=0, J)
HF
(a)
SAMPLE CELL
PUMP FIELD
GAIN
ν
COUPLED ROTATIONAL TRANSITION
PUMP TRANSITION
FORWARD CONFIGURATION
SAMPLE CELL
PUMP FIELD
GAIN
ν
COUPLED ROTATIONAL TRANSITION
PUMP TRANSITION
BACKWARD CONFIGURATION
(b)

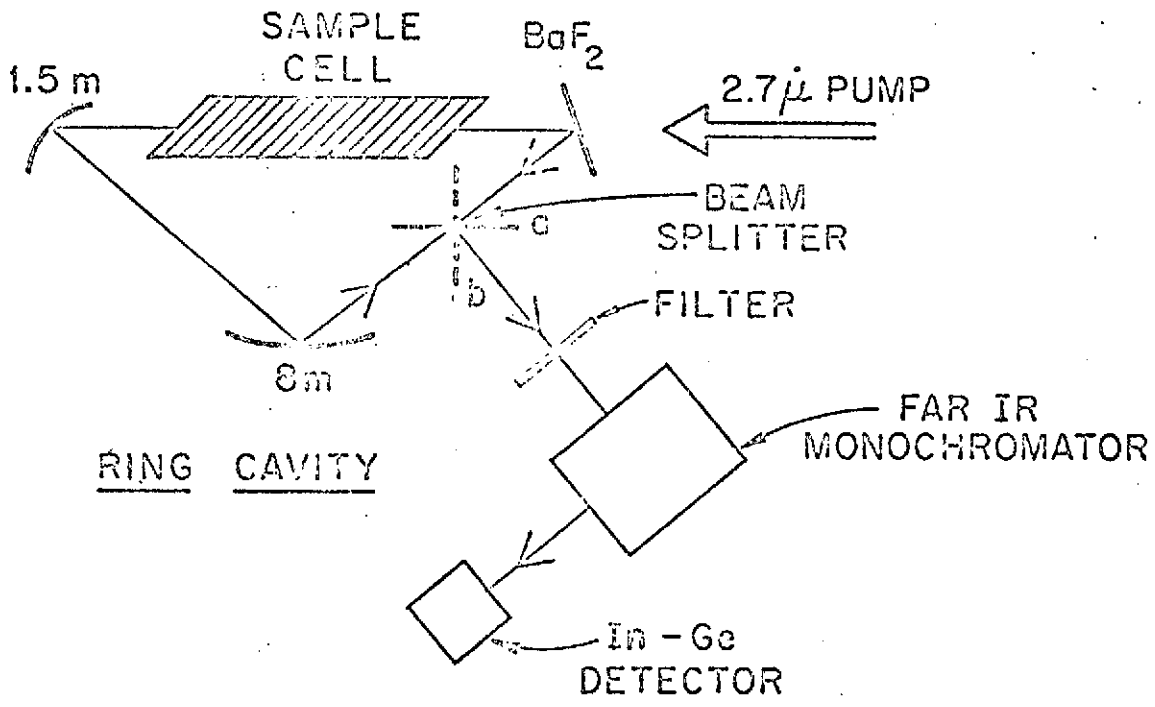
SAMPLE
CELL
BaF_2
1.5 m
2.7μ PUMP
BEAM
SPLITTER
c
b
FILTER
8m
FAR IR
MONOCHROMATOR
RING CAVITY
In - Ge
DETECTOR

PHYSICAL REVIEW A VOLUME 7, NUMBER 1 JANUARY 1973

Selective Reabsorption Leading to Multiple Oscillations in the 8446-Å Atomic-Oxygen Laser*

M. S. Feld, B. J. Feldman,† and A. Javan
Physics Department, Massachusetts Institute of Technology, Cambridge, Massachusetts 02139
and
L. H. Domash‡
NASA Electronics Research Center, Cambridge, Massachusetts 02139
(Received 29 March 1972)

Laser oscillation of atomic oxygen at 8446 Å occurs in four closely spaced lines with peculiar intensity ratios, all detuned from the atomic center frequencies of the three fine-structure transitions. These anomalies are caused by the selective reabsorption of resonance radiation from the lower laser level by ground-state oxygen atoms. The selectivity results from the fact that the velocity distribution of the laser levels is considerably wider than that of the ground state, because of the dissociative mode of production of excited oxygen atoms. Possible extension of this mechanism to the atomic-hydrogen system is discussed. New atomic-oxygen laser lines at 2.89, 4.56, 5.97, 6.86, and 10.40 μ are also reported and assigned.

INTRODUCTION

Although the 8446-Å atomic-oxygen laser was one of the earliest gas lasers to be developed,[1] its behavior has remained mysterious. It was noticed immediately that the laser line was displaced from the peak of the spontaneous-emission profile [Fig. 1(a)], and later, when sufficient gain was obtained, that four laser lines appeared[2,3] with peculiar intensity ratios, all detuned from the atomic center frequencies of the three fine-structure transitions [Fig. 1(b)]. This unique behavior results from the unusual combination of three properties: (i) the fine structure, which consists of pairs of closely spaced transitions sharing a common lower level, (ii) the radiation trapping of the lower level, which is optically connected to the atomic oxygen ground state, and (iii) widely different velocity distributions for the atomic ground state and the lower laser level due to molecular dissociation excitation processes, resulting in resonance reabsorption of radiation over only part of the velocity distribution. The analysis given here explains the occurrence of the four lines and their asymmetrical placement.[4]

In a series of separate but related experiments the coupling among these four laser lines has been investigated. The results and analysis of these experiments are the subject of the following paper.[5]

LEVEL STRUCTURE AND EXCITATION PROCESSES

The level structure of the $3p\ ^3P_{0,1,2}$-$3s\ ^3S_1$ atomic-oxygen laser transitions at 8446 Å is shown in Fig. 2(a), together with the ^3P ground state, which is strongly connected to the $^3S_1$ lower laser level by three fast uv transitions at 1300 Å. The upper laser levels have a radiative lifetime of 36 nsec and the lower level a lifetime of 2.6 nsec.[6,7] The observed fluorescence spectrum due to spontaneous emission from the three upper levels is shown in Fig. 3(a). This measurement confirms the data of Bennett[8] and Tunitsky and Cherkasov,[3] together with an accurate early

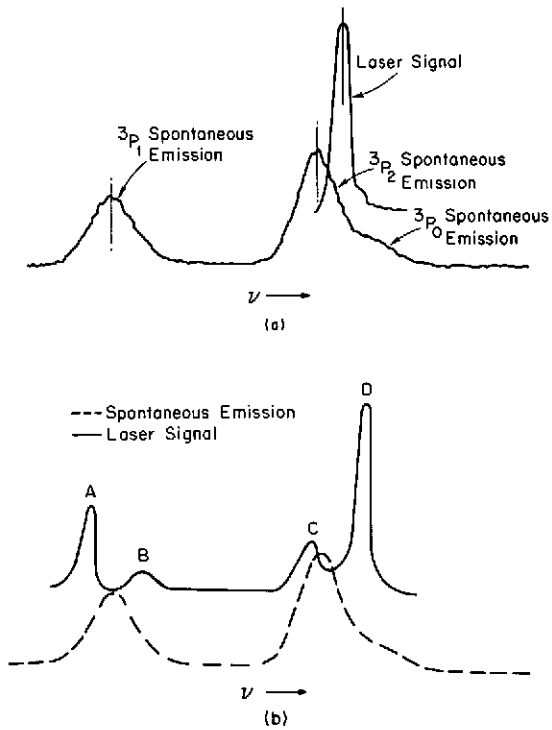

FIG. 1. (a) 8446-Å spontaneous-emission profile, showing initially observed laser line (after Bennett, Ref. 8). (b) 8446-Å spontaneous-emission profile, showing the relative positions of the four laser lines A, B, C, and D.

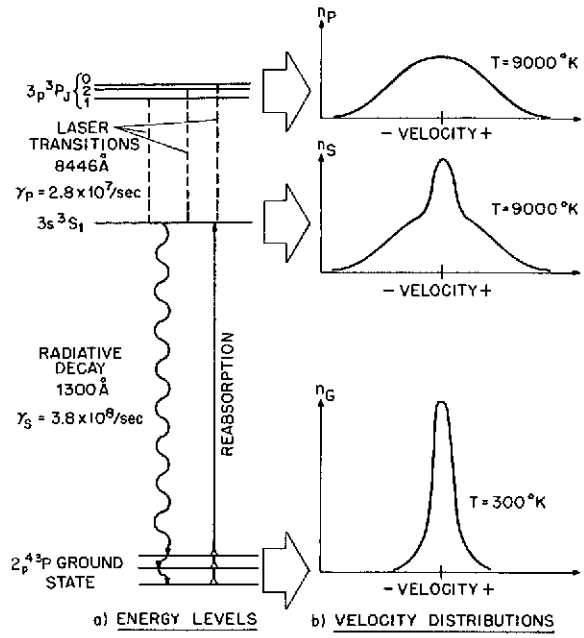

FIG. 2. (a) Relevant atomic-oxygen energy levels, and (b) corresponding velocity distributions, showing selective reabsorption.

study.[9] The $^3P_2$-$^3S_1$ transition is centered 0.557 cm^{-1} higher in frequency than the $^3P_1$-$^3S_1$ transition, and the $^3P_0$-$^3S_1$ transition is 0.159 cm^{-1} above the $^3P_2$-$^3S_1$ transition.[10] The spontaneous-emission intensities of the $J=1, 2, 0$ components are in the ratios of their respective statistical weights, 3:5:1.

Although we are not directly concerned here with the details of the excitation mechanisms, it is necessary to consider their gross features. Low-pressure gas discharges of oxygen mixed with higher pressures of argon as in our experiments have been studied in detail by Bennett *et al.*[1,11] They surmise that oxygen molecules are dissociated in the discharge primarily by metastable argon atoms,

$$\mathrm{Ar}^* + \mathrm{O}_2 \rightarrow \mathrm{Ar} + \mathrm{O} + \mathrm{O}^* + E_{\mathrm{K.E.}}\ , \qquad (1)$$

where O* represents a metastable atomic-oxygen level, and following this, the oxygen metastables are raised to the upper laser levels by electron impact. The energy defect in reaction (1) is several electron volts, giving the excited oxygen atoms a velocity spread considerably wider than that of a room-temperature gas. Presumably, this distribution of velocities is maintained to some extent during the subsequent electron excitation.

Two recent developments in oxygen lasers raise the question of whether this mode of production is the dominant one. First, Tunitsky and Cherkasov have observed laser oscillation at 8446 Å in a pure oxygen discharge cooled to liquid-N_2 temperature.[12] Second, in collaboration with Professor George Flynn, now of Colombia University, we have observed and identified five new cw laser transitions at longer wavelengths in the same argon-oxygen discharge in which laser oscillation at 8446 Å occurs.[13] The energy levels associated with these lines lie considerably higher than the levels of the 8446-Å transition, and the upper level of one transition ($7\,^3D$) cannot easily be excited by electron collisions with the oxygen metastables ($2\,^1D$ and $2\,^1S$). These new transitions are tabulated in Table I.

SELECTIVE RESONANCE REABSORPTION

Whatever the mode of production, measurements of the ^3P-^3S fluorescence spectrum indicate Dop-

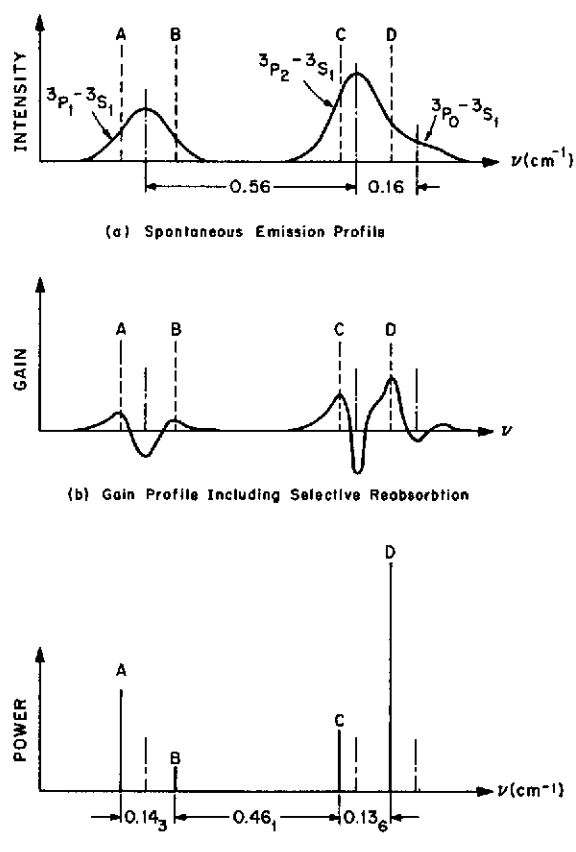

FIG. 3. (a) Spontaneous-emission profile of the three fine-structure transitions at 8446 Å and their measured frequency separations. (b) Sketch of the 8446-Å gain profile. The central portion of each transition is depleted due to selective reabsorption. The slight asymmetry of the $^3P_1$-$^3S_1$ profile is discussed in Ref. 5. (c) Location of the four laser lines relative to their spontaneous-emission profiles. Each line consists of a set of axial modes which extends over a range 0.01–0.05 cm^{-1}. The intensity ratios of the A, B, C lines are shown. The D line is off scale here.

TABLE I. Atomic-oxygen laser transitions.

Observation		Assignment		
	Vacuum	Vacuum	Transition	
Line (μ)	wave numbers (cm^{-1})	wave numbers (cm^{-1})	Upper level	Lower level
0.8446	11 836.29[a]	11 836.335[b]	$3p^3P_J$:	$J=0$
	11 836.16 ± 0.01	11 836.176		$J=2$–$3s^3S^\circ$
	11 835.70	11 835.619		$J=1$
	11 835.55			
2.89	3 456.9 ± 3.0	3 454.90[c]		$4p^3P$–$4s^3S^\circ$
4.56	2192.4 ± 0.9	2192.26		$4p^3P$–$3d^3D^\circ$
6.86	1 458.4 ± 0.5	1 457.75		$5p^3P$–$5s^3S^\circ$
10.40	961.4 ± 0.2	961.26		$5p^3P$–$4d^3D^\circ$
5.97	1 674.9 ± 0.2[d]	1 671.40		$7d^3D^\circ$–$6p^3P$

[a]See text for details.
[b]See Ref. 9.
[c]See Edlen, Ref. 10.
[d]This 0.2% discrepancy may be due to inaccuracy of Edlen's measurement.

pler widths of about 0.145 cm^{-1} full width at half-maximum, corresponding to a velocity distribution of over 9000 °K. In all likelihood the lower laser level also has a broad velocity distribution. In contrast, almost all ground-state oxygen atoms, produced by a variety of collision processes in equilibrium with the walls of the discharge tube, have a room-temperature velocity distribution.

Since resonance photons from the $^3S_1$ lower laser level are heavily reabsorbed, as we shall estimate, within a distance smaller than the tube diameter, atoms in the lower laser level with velocities that are also present in ground-state atoms are effectively inhibited from decaying. As a result, atoms in the central portion of the broad $^3S_1$ velocity distribution have effective lifetimes longer than those in the wings, because of the trapping of their resonance radiation. Consequently, the center population builds up considerably compared to the wings [Fig. 2(b)]. Since the laser gain depends on the population difference between the P and S levels, the final result is to deplete the central portion of the gain profile of each of the three laser transitions over a frequency range determined by the velocity distribution of ground-state atoms.[14] We shall refer to this velocity-dependent process as *selective reabsorption*.[15,16]

Including the fact that radiative decay from the upper laser level goes only to the lower laser level, simple rate equations for the populations of the upper laser n_P and the lower laser levels n_S yield, in the steady state,

$$\frac{n_P}{n_S} = \frac{\gamma_S/\gamma_P}{1+R_S/R_P} \quad , \tag{2}$$

where γ_P and γ_S are the decay rates and R_P and R_S are the net excitation rates. (Note that R_P is most likely much larger than R_S.) At pressures of interest γ_P is approximately A_P, the Einstein spontaneous-emission coefficient.[17] But γ_S is equal to A_S only at the wings of the n_S velocity distribution; at the low velocities where the ground state is heavily populated, resonance photons are trapped and γ_S decreases considerably. Thus γ_S becomes velocity dependent, causing the population inversion to vary across the velocity profile [Eq. (2)]. The corresponding gain profile will be depleted near the atomic-center frequency, and may switch into the absorption phase there. It is even possible, depending on the details of atomic density and temperature, for laser oscillation to occur between two levels whose over-all population inversion, summed over velocities, is zero or negative! This mechanism may well be operative in other molecular dissociation lasers.

A complete treatment of radiation trapping between levels of different velocity distributions is not presently available. Nevertheless, a reasonable estimate which demonstrates the importance of the radiation trapping effect can be obtained from the theory of Holstein,[18] which treats the case of equal velocity distributions. For this purpose the velocity distribution of the $^3S_1$ level may be divided into three regions with respect to u_G, the average thermal velocity of oxygen atoms at room temperature. Over the central portion ($v \ll u_G$), where the ground state is heavily populated, the Holstein theory should predict γ_S with reasonable accuracy. At the wings ($v \gg u_G$) where there are no ground-state atoms, γ_S is given by its untrapped value A_S. In the intermediate region ($v \sim u_G$), γ_S should range between these two values in a slowly varying fashion. A complete theory would, of course, be needed to predict the detailed behavior of γ_S in the intermediate region. The present approach, however, adequately demonstrates the importance of the radiative trapping effect.

According to the Holstein theory, the effective decay rate in the presence of trapping in a long cylinder radius R is given by

$$\gamma_S = 1.60 A_S (n_G \sigma R)^{-1} [\pi \ln(n_G \sigma R)]^{-1/2} \quad , \tag{3}$$

where $n_G \sigma R \gg 1$, n_G is the ground-state density, and σ is the absorption cross section for resonance radiation. The cross section is evaluated from

$$\sigma = \frac{g_S}{g_G} \pi \lambda_0^2 \frac{A_S}{k_0 u_G/\sqrt{\pi}} \quad . \tag{4}$$

Here $k_0 = 1/\lambda_0$ is the propagation constant of the radiation at line center, $k_0 u_G$ is the Doppler width (in units of circular frequency) of ground-state atoms with mass M and most probable speed $u_G = (2kT_G/M)^{1/2}$ and temperature T_G, which we take to be 300 °K. The statistical weights are $g_S = 3$ and $g_G = 9$ in our case. Taking $u_G = 5\times10^4$ cm/sec, $\lambda_0 = (1/2\pi)$ 1300 Å, and $A_S = 380\times10^6$/sec,[6] we find

TABLE II. Splittings (cm^{-1}) between adjacent pairs of the four oxygen laser lines, as reported by various authors. See text for details.

	A-B	B-C	C-D
Patel *et al.*[a]	0.126	0.464	0.130
Feld[b]	0.11	0.48	0.09
Tunitsky and Cherkasov[c]	0.1	0.46	0.1
Present work, pulsed and cw	0.143	0.461	0.136

[a]See. Ref. 2. [b]See Ref. 16. [c]See Ref. 3.

$\sigma \approx 1.2\times10^{-13}$ cm^2.

From this value of σ and the knowledge of the ground-state atomic-oxygen density we can estimate the effect of trapping at the atomic line center. Although we were unable to accurately measure the oxygen pressure in our quasiflow system we estimate it to be at least 100 mTorr. (See discussion in Ref. 5.) Other workers give an optimum value of about 36 mTorr.[1,14] Taking the latter value as a conservative estimate, and assuming as little as 5% dissociation[19] so that $n_G \geq 10^{14}$ cm^{-3}, Eq. (3) with $R = 0.6$ cm yields a decay rate of $\gamma_S \leq 3\times10^7$/sec for low velocity atoms. This quantity increases to the untrapped value of $\sim 4\times10^8$/sec at the wings. We have, then, a lower-laser-level velocity distribution of width ~9000 °K (assuming its Doppler width to be the same as the measured width of the upper laser level) whose central portion is considerably built up over the background population by means of selective reabsorption. Since the upper-level decay rate[6] $\gamma_P = \sim 3\times10^7$/sec, $\gamma_S \leq \gamma_P$ over the region of reabsorption. Accordingly, the n_P/n_S ratio of Eq. (2) is reduced to near or less than unity there, killing the gain. In contrast, at the wings $n_P/n_S \simeq 14$, assuming $R_S \ll R_P$. Thus, the gain profiles of the three 8446-Å transitions will not be proportional to the spontaneous-emission profiles of Fig. 3(a), but instead will have depleted regions at the three line centers, as shown roughly in Fig. 3(b).

INFLUENCE OF SELECTIVE REABSORPTION ON THE OXYGEN FINE-STRUCTURE LASER OSCILLATIONS

Taking into account the overlap of the $^3P_2$-$^3S_1$ and $^3P_0$-$^3S_1$ gain curves, which produce a large combined peak (so that the laser oscillation there is produced by a superposition of gain from the $^3P_0$-$^3S_1$ and $^3P_2$-$^3S_1$ transitions), five gain peaks occur. Oscillation has been observed on all except the smallest ($^3P_0$-$^3S_1$) peak.

The line labeled D in Fig. 3(c) falls on the largest peak and is normally the strongest line. This line, which we find to be displaced 0.12 cm^{-1} above (higher frequency) the $^3P_2$-$^3S_1$ spontaneous-emission peak, was first observed by Bennett, Faust, McFarlane, and Patel,[1] who suggested that the shift was due to an unidentified ozone transition.[20] Shortly afterward, Patel *et al.*[2] observed a quartet of laser lines at 8446 Å in an argon-bromine discharge which was later identified by Tunitsky and Cherkasov[3] as being due to an oxygen impurity and was, therefore, the first observation of the four oxygen lines. Labeling the two $^3P_1$-$^3S_1$ lines as A and B and the remaining line on the low-frequency side of $^3P_2$-$^3S_1$ transition as C [Fig. 3(c)], four lines are observed, spaced as follows: A-B: 0.143 cm^{-1}, B-C: 0.461 cm^{-1}, C-D: 0.136 cm^{-1}. For each line, laser oscillation is observed to extend over a width (excluding the instrumental width of our Fabry–Perot interferometer) of between 0.01 and 0.05 cm^{-1}, the extent of the D line being greatest. This wide range of oscillation is a consequence of the exceptional breadth of the Doppler gain profiles due to the mode of production of excited oxygen atoms, and indicates that a large number of axial modes are simultaneously oscillating. This observation is supported by the fact that a succession of beatnotes between axial modes—out to the response-time limit of our photomultiplier—could be observed on a spectrum analyzer.

The usual relative intensities in a pulsed discharge are as indicated in Fig. 3(c), with the A line second strongest to the D line. A cw discharge produces slightly different ratios, but the spacing between the four lines remains the same within the resolution of our Fabry–Perot interferometer, indicating that at a given pressure the effects of selective reabsorption are not very different for pulsed and cw discharges.

As can be seen from Fig. 3(c), line A is always stronger than line B. Furthermore, it is found that lines A and B are placed slightly asymmetrically about the $^3P_1$-$^3S_1$ spontaneous-emission profile. These small asymmetries are discussed further in Ref. 5.

If our explanation of the depleted central region is correct, the width of this zone and therefore, the laser line spacing, should be sensitive to the oxygen partial pressure through the n_G dependence of Eq. (3). Higher oxygen pressures should enlarge the depleted region. Indeed, our data were taken at a considerably higher O_2 pressure than that of Patel *et al.*[2] and, as shown in Table II, our line splittings change relative to theirs in the expected direction: A and B are further apart, B and C are slightly closer together, and the C-D separation, which undergoes influences in opposite directions from the $^3P_2$-$^3S_1$ and $^3P_0$-$^3S_1$ transitions, increases, but less so than A-B. Tunitsky and Cherkasov[21] observed a 3-GHz shift in the position

of the D line by varying the O_2 pressure over a decade.

POSSIBLE APPLICATIONS TO OTHER SYSTEMS

The mechanism which leads to laser oscillation in atomic oxygen has wide potential applicability in other gas-laser systems. What is required is that the velocity distribution of the upper laser level be broader than that of the lower level so that with appropriate level lifetimes, population inversion can occur at the wings of the distribution even though inversion is not possible at the center. A possible system in which gain may be produced in this way is the H_α line of atomic oxygen at 6563 Å[22] in a H_2-Ne discharge cooled to liquid-N_2 temperature. In this case "hot" hydrogen atoms are produced in the $n=3$ state by the reaction

$$H_2 + Ne^* \rightarrow Ne + H + H_{n=3} + 0.05\ eV\ , \qquad (5)$$

with a cross section of $\sigma = 1.4\times10^{-15}$ cm^2.[23,24] As explained above, cooling the discharge should narrow the velocity distribution of the $n=2$ level without affecting the corresponding width of the $n=3$ level.

We have studied the hydrogen system utilizing standard absorption techniques to measure the neon metastable population as a function of gas pressure and discharge current, while at the same time monitoring the spontaneous-emission intensity of the H_α, H_β, and H_γ lines. The details of the experiment will be prepared for publication at a later time. The results indicate that in a 1-Torr neon discharge with 20 mTorr of H_2 at low currents (~12 mA), so as not to dissociate too much H_2 by electron collisions, a population inversion of about 4×10^7/cm^3 occurs at the wings of the $3P_{5/2}$-$2P_{3/2}$, H_α transition. The gain of the system is estimated to be about 0.5% per meter, so that for laser oscillation a discharge tube several meters long would be required.

Other possible laser systems based on this effect are also under consideration.

ACKNOWLEDGMENTS

We would like to thank Professor Victor George for a useful discussion on plasma parameters. This paper is dedicated to the memory of Jerry Adler, whose enthusiasm and energetic assistance gave the experiment an effective start.

---

*Work supported in part by the National Aeronautics and Space Administration and NASA Electronics Research Center.

†Present address: Los Alamos Scientific Laboratory, Los Alamos, N. M. 87544.

‡National Research Council Postdoctoral Research Associate. Present address: Maharishi International University, Rishikesh, India.

[1]W. R. Bennett, Jr., W. L. Faust, R. A. McFarlane, and C. K. N. Patel, Phys. Rev. Letters 8, 470 (1962).

[2]These four lines were initially attributed to bromine: C. K. N. Patel, R. A. McFarlane, and W. L. Faust, Phys. Rev. 133, A1244 (1964).

[3]L. N. Tunitsky and E. M. Cherkasov, J. Opt. Soc. Am. 56, 1783 (1966); Opt. i Spektroskopiya 23, 287 (1967) [Opt. Spectry. 23, 154 (1967)].

[4]L. Domash, M. S. Feld, B. J. Feldman, and A. Javan, Bull. Am. Phys. Soc. 16, 593 (1971).

[5]L. H. Domash, B. J. Feldman, and M. S. Feld, following paper, Phys. Rev. A 7, 262 (1973).

[6]W. L. Wiese, M. W. Smith, and B. M. Glennon, *Atomic Transition Probabilities*, Dept. of Commerce, Natl. Bur. Stds. (U.S. GPO, Washington, D. C., 1966), Vol. I.

[7]Upper-level lifetime: see, for example, J. Solarski, and W. L. Wiese, Phys. Rev. 135, A1236 (1964). Lower-level lifetime: see, for example, A. B. Prag and K. C. Clark, Phys. Rev. Letters 12, 34 (1964). These and other references are contained in Ref. 6.

[8]W. R. Bennett, Jr., *Proceedings of the Third International Conference on Quantum Electronics* (Dunod Cie, Paris, 1963).

[9]D. O. Davis and K. W. Meissner, J. Opt. Soc. Am. 43, 510 (1953).

[10]The partially inverted order of the ^3P fine-structure multiplet is due to configuration mixing: B. Edlen [Kgl. Svenska Vetenskapsakad. Handl. 20, 10 (1943)]; E. U. Condon and G. H. Shortley, *The Theory of Atomic Spectra* (Cambridge U.P., London, 1959).

[11]W. R. Bennett, Jr., Appl. Opt. 1, 24 (1962).

[12]L. N. Tunitsky and E. M. Cherkasov, Zh. Tekh. Fiz. 38, 1200 (1968) [Sov. Phys. Tech. Phys. 13, 993 (1969)].

[13]G. W. Flynn, M. S. Feld, and B. J. Feldman, Bull. Am. Phys. Soc. 12, 669 (1967).

[14]The issue of different velocity distributions in oxygen was first raised, in a somewhat different context, by S. G. Rautian and P. L. Rubin [Opt. i Spektroskopiya 18, 326 (1965) [Opt. Spectry. 18, 180 (1965)]]. See also L. N. Tunitsky and E. M. Cherkasov, Opt. i Spektroskopiya 26, 630 (1969) [Opt. Spectry. 26, 344 (1969)].

[15]M. S. Feld, B. J. Feldman, and A. Javan, Bull. Am. Phys. Soc. 12, 669 (1967).

[16]M. S. Feld, Ph.D. thesis (MIT, 1967) (unpublished).

[17]Strictly speaking, at operating pressures collision broadening contributes to the γ's. In the present discussion, however, this contribution may be safely neglected, since the collision rate is much smaller than A_S. See Ref. 5 for further discussion.

[18]T. Holstein, Phys. Rev. 72, 1212 (1947); 83, 1159 (1951).

[19]This figure is conservative and is consistent with the microwave data of F. Kaufman and J. R. Kelso [J. Chem. Phys. 32, 301 (1960)] and our own estimates.

[20]Other experimental data, reported in Ref. 5, indicate the existence of a second shift, smaller than that due to the selective reabsorption effect discussed here. The shift is possibly attributable to the presence of O^{18} in natural abundance. (See Ref. 5 for details.) It is emphasized, however, that the shifts and line placements described here are predominantly due to selective reabsorp-

tion and overlap, as discussed above.

[21]L. N. Tunitsky and E. M. Cherkasov, Zh. Tekh. Fiz. 37, 2038 (1967) [Sov. Phys. Tech. Phys. 12, 1500 (1968)].

[22]Bennett (Ref. 8) attempted to obtain oscillation on the 6563-Å H_α line, but was unable to obtain laser oscillation in a 3-m Ne-H_2 discharge. He did not, however, take advantage of reaction (5) in regard to the excess kinetic energy supplied to the atoms produced in the $n=3$ state. We propose to do this by cooling the discharge tube.

[23]T. Marshall, J. Appl. Phys. 36, 712 (1965).

[24]Recently, J. A. McInally [Bull. Am. Phys. Soc. 15, 431 (1970)] proposed that hydrogen atoms in the $n=3,4,5$ states are selectively produced in a neon discharge by the two-step reaction:

$$Ne^* + H_2 \rightarrow Ne + H_2^{*\nu} + e,$$

$$H_2^{*\nu} + e \rightarrow H^* \ (n=3,4,5) + H + E_{K.E.}.$$

This mechanism is consistent with the recently observed "superradiant" laser oscillations at 4861.2 and 4340.6 Å tentatively assigned to the H_β and H_γ lines. See G. J. Dezenberg and C. S. Willett, IEEE J. Quantum Electron. QE-7, 491 (1971). Similar processes may also play an important role in producing atomic-oxygen laser oscillations observed in a Ne-O_2 discharge.

PHYSICAL REVIEW A VOLUME 7, NUMBER 1 JANUARY 1973

Interactions among Multiple Lines in the 8446-Å Atomic-Oxygen Laser*

L. H. Domash†
NASA Electronics Research Center, Cambridge, Massachusetts

and

B. J. Feldman‡ and M. S. Feld
Physics Department, Massachusetts Institute of Technology, Cambridge, Massachusetts 02139

(Received 29 March 1972)

The atomic-oxygen laser oscillates at four closely spaced frequencies on the gain profile of the 8446-Å fine-structure transitions. A set of experiments is reported which studies the competition among these four lines by suppressing one of them. The results are explained on the basis of the interaction of laser lines oscillating on Doppler-broadened transitions sharing a common lower level.

I. INTRODUCTION

The atomic-oxygen laser oscillates at four closely spaced frequencies on the atomic gain profile of the 8446-Å fine-structure transitions ($3p^3P_{1,2,0} - 3s^3S_1$). In the preceding paper[1] it was explained that because of *selective reabsorption* of uv resonance radiation emanating from the lower laser level, the gain is depleted at the central portion of each fine-structure transition, and laser oscillation occurs only at the *wings* of the two fine-structure transitions with highest gains. Figure 1 illustrates again the positions of the four laser lines relative to the spontaneous-emission profile of the three fine-structure transitions. These lines are labeled A, B, C, and D in order of increasing frequency, with A and B falling on opposite sides of the $^3P_1 - {}^3S_1$ transition, and C and D falling on opposite sides of the $^3P_2 - {}^3S_1$ transition. Line D is largest due to overlap of the high-frequency wing of the $^3P_2 - {}^3S_1$ transition and the low-frequency wing of the $^3P_0 - {}^3S_1$ transition.

The present paper reports a set of experiments which studies the interactions among the four laser lines by suppressing one of them (in a manner to be described below) and observing the intensity changes of the other three. It is found[2] that suppressing the strongest line D causes line C to greatly increase in intensity, line B to increase somewhat, and line A to decrease. This is illustrated in Figs. 2(a) and 2(b), which show scanning Fabry–Perot interferometer traces of the four laser lines. Similarly, blocking line C causes line A to increase in intensity and line B to de-

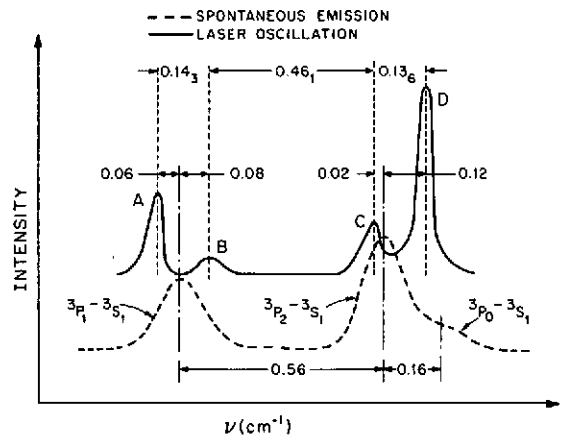

FIG. 1. The four laser lines near 8446 Å showing positions relative to the spontaneous emission of the three fine-structure transitions.

crease in intensity. [Compare Figs. 2(a) and 2(c).] Similar effects occur when lines A or B are suppressed.

It will be shown in this paper that these interactions result from two facts: (i) The laser oscillations on the $^3P_2 - {}^3S_1$ and $^3P_1 - {}^3S_1$ transitions, which share a common level, are coupled at certain frequencies and compete; (ii) there is a small additional line-shape asymmetry which, in the $^3P_1 - {}^3S_1$ transition, causes the A and B lines to be slightly asymmetrically placed with respect to the $^3P_1 - {}^3S_1$ center frequency (Fig. 1).

The paper is divided as follows: The experimental setup is described in Sec. II. Section III, which discusses laser oscillations on coupled transitions, is subdivided into three parts: A, an explanation of the laser-induced line-narrowing effect; B, its application to the atomic-oxygen laser; and C, an explanation, based on A and B, of the experimental observations. In Sec. IV the asymmetrical placement of the laser lines is discussed. Some interesting competition effects expected at lower operating pressures are discussed in Sec. V. Section VI is the conclusion.

Some additional experimental information on the pulsed-laser system is deferred to the Appendix.

II. EXPERIMENT

Most of the experimental work reported here was done separately on two versions of the oxygen laser, one using a continuous direct-current discharge, and the other a high-voltage pulsed discharge. The two systems behaved very much alike with respect to the phenomenon of interest in this paper, and differed mainly in that the pulsed system had a higher over-all gain. Most of our discussion will treat the data taken with cw and pulsed lasers as similar unless otherwise noted. Details of the pulsed system are deferred to the Appendix.

A 1.5-m quartz discharge tube of 12-mm in diam. with hot cathode and a water-cooling jacket was used. The optical resonator consisted of two 2-m radius mirrors spaced by 2 m (confocal), or one 2-m and one flat mirror (hemispherical). With a pulsed discharge (voltage: 20 kV; pulse duration: 1.8 μsec; repetition rate: 2500–3000 pulses/sec), external mirrors of reflectivity 99.2% and 98.5% would suffice to have all four lines lasing, but with a cw discharge (optimum current: 180–220 mA) a combination of 99.8% and ~100% reflectivity mirrors were required, one of which was internal, to obtain oscillation on four lines.

Because oxygen was very heavily adsorbed onto the walls and cathode of our tube, we found it difficult to maintain statically the optimum pressure of oxygen reported by other workers (36 mTorr of O_2 in 1.3 Torr of Ar according to Bennett *et al.*[3]), and instead arrived at the following method: The tube was filled with 1 Torr of argon, and a reservoir was filled with an equal pressure of oxygen. When a connecting valve was opened, oxygen would diffuse through the argon and collect on the tube walls, resulting effectively in a flowing-oxygen system. Unfortunately, we are left without accurate knowledge of the resulting oxygen pressure in the active region; it is estimated to be at least 100 mTorr, somewhat higher than the values quoted by other workers.[3,4] This system would break into oscillation after "cooking" for about 5 min (presumably the time to establish a certain atomic-oxygen density by means of dissociation), and would then run for about 10 min before losing gain.

All the laser-line spectra and also the spontaneous-emission profile were observed with a piezoelectrically scanned Fabry–Perot interferometer having a free spectral range of 1.16 cm^{-1} and a finesse of about 40, for a resolution of 0.03

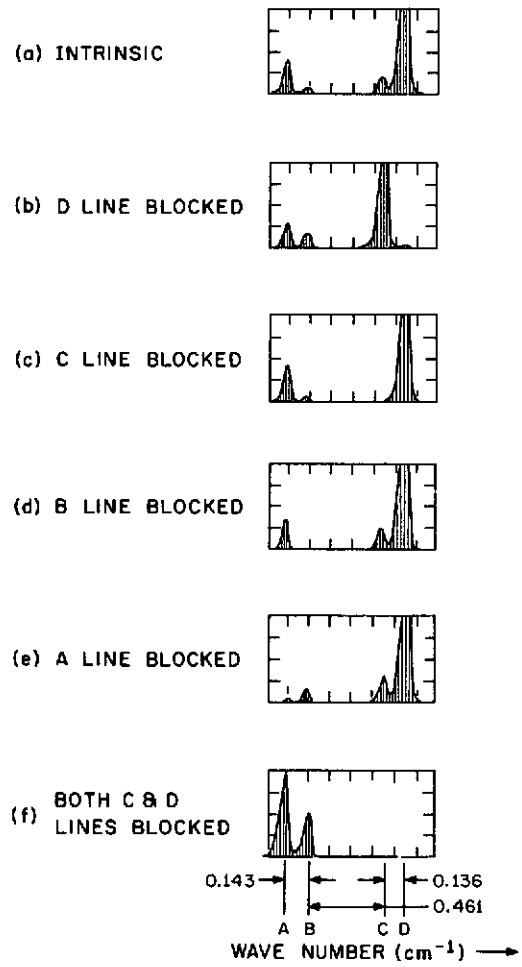

FIG. 2. Oscilloscope traces of Fabry–Perot scans showing the laser output behavior when one of the four laser lines is selectively blocked.

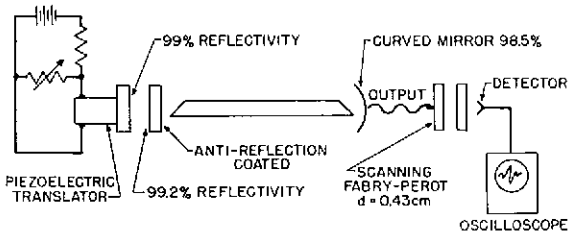

FIG. 3. Optical cavity using Fabry–Perot interferometer as one end mirror. This arrangement can selectively block oscillation of the four laser lines, one at a time.

cm^{-1}.

Interactions of the four laser lines were studied with a special arrangement at one end of the cavity, illustrated in Fig. 3. The flat mirror of the hemispherical cavity was replaced by a Fabry–Perot interferometer consisting of a pair of flats each coated for 99% reflectivity at 8446 Å. The inside flat mirror was antireflection coated on the side toward the Brewster window, and the outside flat could be translated by means of a piezoelectric mount. The free spectral range of this "end cavity" was 1.32 cm^{-1}. As a part of the over-all optical cavity, this device acted as a very high reflectivity mirror (> 99.9%) except over narrow spectral regions of high transmission 0.03 cm^{-1} wide and spaced 1.32 cm^{-1} apart. These narrow regions of resonant transmission became "rejection notches" for the laser cavity, and their positions could be manually adjusted by varying the dc voltage on the translator. It was thus possible to tune the end cavity so as to selectively block the oscillation of any one of the four laser lines A, B, C, or D. (Adjacent rejection notches fell 1.32 cm^{-1} away where they had no effect.)

The results (Fig. 2), described briefly in the Introduction, will be more fully discussed in Sec. IV in conjunction with the explanation of the effect. However, one important additional result should be noted here: By narrowing the spacing of the end-mirror etalon to 1 mm we were able to make a rejection notch broad enough to simultaneously block oscillation on *both* C and D, thus allowing A and B to be seen free of their influence. The result is shown in Fig. 2(f), where it is seen that A remains about twice as big as B. This residual asymmetry is indicative of a small asymmetry in the $^3P_1 - {}^3S_1$ gain profile. Such an asymmetry is also sugested by the asymmetrical placement of the A and B lines with respect to the $^3P_1 - {}^3S_1$ atomic-center frequency (Fig. 1), already mentioned in the Introduction. (It should be noted that the positions of the A and B lines are unchanged when lines C and D are suppressed.) The existence of this asymmetry, further discussed in Sec. IV, is important to a complete understanding of the experimental results.

III. LASER OSCILLATION ON COUPLED TRANSITIONS

A. Laser-Induced Line-Narrowing Effect

The line shape of a Doppler-broadened transition is dramatically altered by the presence of an intense standing-wave laser field resonating with a second Doppler-broadened transition sharing a common level. The standing-wave field selectively interacts with atoms whose velocities Doppler shift one of its traveling-wave components into resonance. This produced changes in the level populations over two narrow intervals symmetrically located about the center of the velocity distribution. These changes reflect themselves in the gain profile of the coupled transition, scanned by means of a weak monochromatic probe field colinear with the standing-wave field: Two narrow Lorentzian resonances appear superimposed upon the broad background signal at frequencies symmetrically located about the corresponding line center. This phenomenon, called laser-induced line narrowing, has been treated extensively by several authors.[5]

The situation is illustrated in Fig. 4 for the case of a common lower level. A laser oscillation which is displaced (for some reason) from its atomic line center ω_2 to a frequency $\omega_2 + \delta$ will produce gain depletions in four different regions:

(a) the gain immediately about laser oscillation will be depleted. The extent of the depletion does not concern us here.[6]

(b) the gain on the opposite side of the same transition will be depleted over a Lorentzian profile, centered at $\omega_2 - \delta$, of width (full width at half-maximum in units of circular frequency)

$$\Gamma_L = \gamma_L + \gamma_2 \ , \tag{1}$$

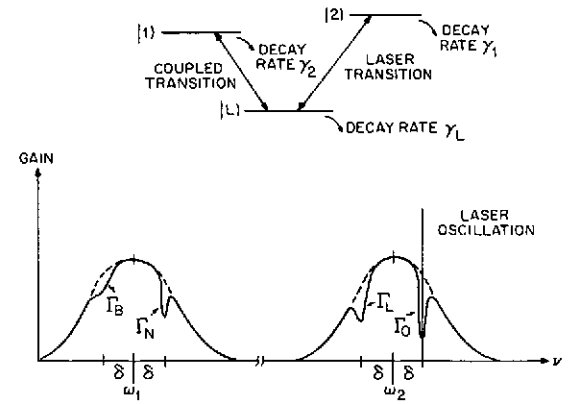

FIG. 4. Gain depletions produced by a standing-wave laser field interacting with coupled Doppler-broadened transitions.

where γ_2 and γ_L are the relaxation rates of the upper and lower levels of the laser transition, respectively, as determined by radiative decay and collisions. This effect is well known.[7]

(c) On the *coupled* transition, whose atomic-center frequency is ω_1, there will be a *narrow* zone of gain depletion centered at $\omega_1+\delta$, Lorentzian in shape, of width

$$\Gamma_N=\gamma_1+\gamma_2 \tag{2}$$

(in the special case of transitions of approximately equal frequencies, the case which concerns us here).

(d) Finally, on the opposite side of the coupled transition, at frequency $\omega_1-\delta$, there will be a *broad* gain dip, also Lorentzian in shape, of width

$$\Gamma_B=\gamma_1+\gamma_2+2\gamma_L \ . \tag{3}$$

So the difference between Γ_B and Γ_N is twice the "width" of the lower level. If the lower level is relatively broad, which is usually the case in laser transitions, Γ_B and Γ_N can be observably different. Such observations have been made recently by several workers[8-10] in different experimental contexts.

It is important to notice that these gain depletions can differ considerably in magnitude from one another. The area (gain×frequency) of the Γ_L dip is usually much larger than the areas of the Γ_N and Γ_B dips, which are equal to each other. The ratio of the areas is given by

$$\frac{\text{area of } \Gamma_N \text{ or } \Gamma_B}{\text{area of } \Gamma_L}=\frac{\gamma_2}{\gamma_2+\gamma_L}\,\frac{|\mu_1|^2}{|\mu_2|^2}\ , \tag{4}$$

where μ_j is the matrix element connecting levels j and L.

In regard to the relative positions of the gain depletions (Fig. 4) the Γ_L dip is always positioned symmetrically across the laser gain profile from the laser frequency, the narrow dip is always located a frequency interval δ above (below) the atomic line center of the coupled transition as the laser oscillates δ above (below) its line center, and the broad dip Γ_B is always symmetrically located across the gain profile from Γ_N. If the laser oscillates at the atomic-center frequency ($\delta=0$), the broad and narrow dips on the gain profile of the coupled transition will coalesce.[11]

In case several laser modes are simultaneously oscillating, as in the oxygen laser, each one will produce its own set of depletions. Then the gain profile depletions will take the form of combs of adjacent dips.

B. Application to Atomic Oxygen

As explained above, the atomic-oxygen laser not only has closely spaced transitions sharing a common lower level, but in addition has its laser oscillations intrinsically displaced from the atomic line centers because of the selective reabsorption mechanism that greatly depletes the gain there.[1,12] So the broad and narrow depletions in the gain profiles of coupled transitions should be well separated. Thus, at certain frequencies, the four oxygen laser lines should interact in gain and compete with one another. This has been clearly observed in our experiments.

Figure 4 should now be interpreted as a simplified picture of one part of this effect in the oxygen laser. If we identify the $^3P_2-{}^3S_1$ transition as the ω_2 transition and the $^3P_1-{}^3S_1$ transition as ω_1 [so that $(\omega_2-\omega_1)\approx 17$ GHz], then the laser line illustrated corresponds to the main and strongest laser oscillation, denoted as the D line in Fig. 1. (Note that the depleted centers due to selective reabsorption have not been shown in Fig. 4.) The displacement of the D line above the $^3P_2-{}^3S_1$ atomic line center was measured by Patel *et al.*[13] to be 0.07 cm^{-1} and in our present experiments, at higher pressures, we find this displacement to be 0.12 cm^{-1}.

The full manifestation of these gain interactions in oxygen via the broad and narrow dips is evidently quite complicated. Each of the four lines A, B, C, D produces a gain dip Γ_L on the other side of its own gain profile, and a broad Γ_B dip and a narrow Γ_N dip on the other transition, all placed according to the simple rules already stated. However, the fact that the D line is much stronger than A, B, or C leads to a basically simple experimental situation.

The linewidths for Γ_L, Γ_N, and Γ_B are given by Eqs. (1)–(3) and depend upon the relaxation rates γ_1, γ_2, and γ_L. The known radiative widths are $\gamma_1=\gamma_2=4.5$ MHz and $\gamma_L=60.5$ MHz.[14,15] At gas mixtures of approximately 1-Torr collisions contribute an additional 5–10 MHz to the decay rates. (The exact value is not critical.) Therefore, the expected linewidths are

$$\begin{aligned}\Gamma_L&\approx\gamma_L+\gamma_2\simeq 80 \text{ MHz},\\ \Gamma_N&\approx\gamma_1+\gamma_2\simeq 25 \text{ MHz},\\ \Gamma_B&\approx\gamma_1+\gamma_2+2\gamma_L\simeq 150 \text{ MHz}.\end{aligned} \tag{5}$$

As explained above, the D line—the most intense line—consists of a set of adjacent longitudinal modes spanning over 0.05 cm^{-1}. Consequently, the D line produces a set of Γ_N dips on the $^3P_1-{}^3S_1$ (ω_1) transition in the vicinity of the B line (Fig. 4). Since the axial mode spacing of our 2-m laser is 75 MHz, these narrow dips tend to run together in a sawtooth pattern rather than remaining a comb of distinct holes. Continuing to refer to Fig. 4, the D line also produces a set of Γ_L dips on the $^3P_2-{}^3S_1(\omega_2)$ transition near the C line, and a set of Γ_B dips on the $^3P_1-{}^3S_1(\omega_1)$ tran-

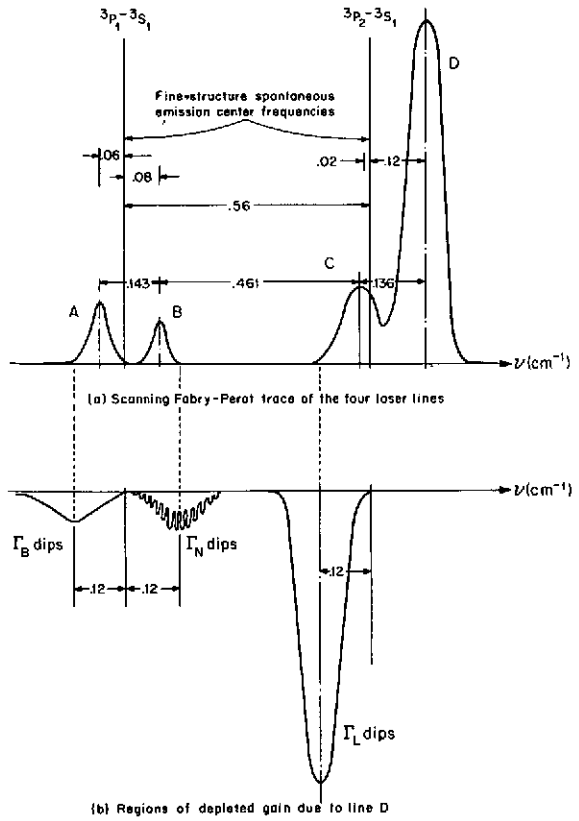

FIG. 5. Fabry-Perot scan of laser lines A, B, C, D (shown upwards) compared to expected gain dips due to line D alone (shown downward).

sition near the A line. Since the width of the Γ_L and Γ_B dips is broader than the laser-mode spacing, each set of dips runs together, depleting broad regions of the respective gain profiles.

The three over-all gain depletions differ considerably in magnitude: Since $\gamma_L \approx 5\gamma_2$, the over-all Γ_L depletions near line C are about six times as deep as the Γ_N depletions near line B [Eq. (4)]. It is seen from Eqs. (5) that the Γ_B dips are about six times broader than the Γ_N dips. But the areas of Γ_N and Γ_B are equal, and the combs of Γ_N dips have peaks and valleys such that their average value is about equal to the value of the broad flat region of depletion produced by the multiple overlapping Γ_B dips.

The over-all situation is represented in Fig. 5. Figure 5(a) shows a Fabry–Perot scan of lines A, B, C, and D all oscillating together. Note the large extent of laser oscillations at D, the relative intensities, and especially the placement of the four lines relative to the line centers of the two main fine-structure components. Line D is centered about 0.12 cm^{-1} above the $^3P_2 - {}^3S_1$ center frequency, whereas line C is only 0.02 cm^{-1} below it. Lines A and B fall 0.06 cm^{-1} below, and 0.08 cm^{-1} above the $^3P_1 - {}^3S_1$ center frequency, respectively.

Figure 5(b) is a sketch showing the positions, extent, and relative strengths of the gain depletions due to line D only (drawn extending downward). The widths and relative strengths are roughly to scale: The Γ_L dips are about six times stronger than the Γ_N and Γ_B dips, and the Γ_N and Γ_B dips have equal average values.

The balance of expected interactions is clear from this picture. First, because of its large extent (and the fact that Γ_L dips are quite deep), line D can heavily suppress line C, despite the fact that the Γ_L dips are centered quite far (0.10 cm^{-1}) from the center of line C. Second, line D also suppresses both lines A and B through the Γ_B dips and Γ_N dips, respectively. However, line B is suppressed more, since the Γ_N dips are centered closer to the peak of line B (0.04 cm^{-1}) than the Γ_B dips to line A (0.06 cm^{-1}). We are now prepared to understand the results pictured in Fig. 2.

C. Line Interactions

Taking into account the three kinds of dips produced by the D line, and noting their relative strengths, where they fall relative to lines A, B, and C (Fig. 5), and the asymmetrical placement of lines A and B about the $^3P_1 - {}^3S_1$ center frequency, we can now account for the experimentally observed intensity changes. As described earlier in Sec. II, by varying the spacing of the end-mirror cavity, we could inhibit oscillation on one line, and in doing so also remove the Γ_L, Γ_N, and Γ_B dips it produces. The resulting intensity changes could be clearly observed.

The results are shown in Fig. 2 which uses the data from the pulsed system. The cw data were entirely similar, except that the intensity ratios of the four lines were slightly different. Figure 2(a) shows the intrinsic situation, with the spectral position of the rejection notch placed away from the four laser lines. In Fig. 2(b) oscillation of the D line is prevented by placing the transmission resonance of the end cavity at the spectral position of D. As discussed above, line D heavily suppresses line C even though C lies in the wing of the Γ_L dips due to D. The Γ_N dips of line D suppress line B more than the Γ_B dips do line A. Hence, upon suppressing line D, and thus removing the gain dips it produces, both lines C and B are expected to increase in strength. As line B grows, line A should decrease, since A and B compete through their own Γ_L dips and line B's Γ_L dip (near A) increases as B rises.

This is exactly what is seen in Fig. 2(b), where line D is "blocked," and line C, ordinarily weak, jumps to an intensity almost equal to that of the

old D line. The intensity of line B increases about 90%, and that of line A falls off.

As line C grows, the Γ_L, Γ_N, and Γ_B dips associated with *it* grow too and become important. Note that the placement of the Γ_N and Γ_B dips due to line C tends to reinforce the increase of line B and the decrease of line A. Of course, the dips due to line C are weakly present even when C has its smaller initial value.

In Fig. 2(c) the oscillations of line C are blocked. D gets a bit stronger, thus depressing B, and A gains 50% in intensity over the intrinsic value because the Γ_N dips due to C are lifted, depressing B further. In general the A line tends to increase and decrease in strength along with the D line, and the B line changes up or down as the C line does.

Figures 2(d) and 2(e) show, for completeness, the effects of blocking the B and A lines. Blocking the B line enhances A over its intrinsic strength by removing the Γ_L dip due to B. Blocking the A line enhances B and also slightly enhances C. This demonstrates that the A line produces small dips back on the $^3P_2 - {}^3S_1$ transition, as expected.

All of these interactions can be understood by the above considerations. The weak $^3P_0 - {}^3S_1$ transition can be neglected except that it is the source of asymmetry that causes D to be generally favored over C in two separate ways: First, D enjoys gain from both the upper $^3P_2 - {}^3S_1$ wing and the lower $^3P_0 - {}^3S_1$ wing; second, the tails of a set of Γ_N dips due to D oscillating on the low-frequency wing of the $^3P_0 - {}^3S_1$ transition react back on the low-frequency wing of the $^3P_2 - {}^3S_1$ transition (near the C line) to further depress the gain there. (Angular momentum selection rules forbid three-level interactions between the $^3P_0 - {}^3S_1$ and $^3P_1 - {}^3S_1$ transitions for fields of the same polarization, as in our Brewster-window system.)

IV. ASYMMETRIC PLACEMENT OF THE LASER LINES

In the experiments described above we have found line D to interact more strongly with line A than with line B. Similarly, line C is found to interact more strongly with line B than with line A. Our explanation of this preferential coupling is based upon small asymmetries observed in the intensities of lines A and B and in their relative displacements from the $^3P_1 - {}^3S_1$ spontaneous-emission center frequency. These asymmetries are observed even when both lines C and D are prevented from oscillating. Figure 2(f), which is a Fabry–Perot scan of lines A and B oscillating with C and D both blocked, clearly shows the intensity asymmetry. A careful comparison of Fig. 2(f) with Fig. 2(a), the intrinsic situation (all lines free to oscillate), shows that the A-B positions are unchanged when lines C and D are suppressed, and the "residual" asymmetry in the displacements of lines A and B is the same as that shown in Fig. 1.

The cause of this asymmetry is uncertain. It cannot be due to overlap as in the case of the C-D lines, where the $^3P_0 - {}^3S_1$ low-frequency wing contributes to the gain of the D line. A tentative explanation is the presence of O^{18}, which has a natural abundance of 1:500. The isotope shift of the O^{18} transitions at 8446 Å is quite large, about 0.14 cm^{-1} to the high-frequency side of the O^{16} transitions,[16] and is comparable to the observed Doppler widths (full width at half-maximum ~ 0.15 cm^{-1}).[1] Accordingly, the O^{16} gain profile at each fine-structure component is modified by a small O^{18} component, displaced about half a linewidth upward in frequency. As explained in Ref. 1, the central portion of each O^{16} fine-structure gain profile is in the absorbing phase.[12] Estimates based on the density of atomic O^{18} similar to those given in Ref. 1 indicate that the centers of the O^{18} fine-structure gain curves also may be depleted, producing a small reduction at the high-frequency wing of each fine-structure gain profile, but leaving the low-frequency wings unaffected. This asymmetry would be most noticeable in the $^3P_1 - {}^3S_1$ fine-structure transition, and is probably masked by overlap effects in the other components. The slight asymmetry would be intensified by the regenerative effects of laser oscillation.

At any rate, further studies, such as variation of the O^{18} abundance, will be necessary to ascertain the detailed causes of the line-shape asymmetry.

V. COMPETITION EFFECTS AT LOWER OXYGEN PARTIAL PRESSURE

It should be pointed out that our results may be quite specific to the oxygen concentrations (over 100 mTorr) used in our experiments. Earlier observers,[3,17,18] working at lower oxygen partial pressures (Bennett *et al.*, Ref. 3, quote an optimum value of 36 mTorr) found a considerably smaller displacement of the D line (about 0.07 cm^{-1} instead of our value of 0.12 cm^{-1}). This smaller displacement is expected from the considerations of Ref. 1. Furthermore, at lower pressures the $^3P_1 - {}^3S_1$ line-shape asymmetry (which causes the A-B asymmetries) discussed in Sec. IV might be reduced. Therefore, the Γ_B and Γ_N dips produced by line D would be more closely centered on lines A and B, respectively, as compared to the higher-pressure case studied in this paper. Also, the separation between line A and the center of the Γ_B dips would be closer to that between line B and the Γ_N center. Thus, the asymmetry which, at high pressures, makes the Γ_N dips more influential than the Γ_B dips would be reduced if not entirely

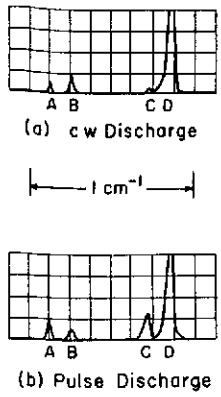

FIG. 6. Oscilloscope traces of Fabry-Perot scans for the four laser lines, comparing the cw (a) and pulsed (b) behavior. In the pulsed trace about 200 individual pulses occur during a scan. The horizontal scale is 0.127 cm^{-1}/div. The vertical scales in (a) and (b) differ by about an order of magnitude. In both cases the D-line intensity is off scale.

removed.

We would, in this case, expect another aspect of the line-narrowing effect to manifest itself. If the Γ_N and Γ_B dips of line D were more or less centered on the lines A and B, respectively, then the modes oscillating on line B would be sensitive to the comb of individual gain depletions within the Γ_N region. If the modes fell on the peaks of the depletions, then oscillation at B would tend to be suppressed; if the modes fell between the peaks the suppression effect would be diminished. At A, on the opposite side of the $^3P_1 - {}^3S_1$ gain profile, there would be no such effect, since the individual Γ_B gain depletions are much wider than those of Γ_N and completely run together. The resulting competition between lines A and B would depend on the relative placement of the modes of line B with respect to the Γ_N dips—line A would dominate when the B modes fell on the depletion peaks, line B would dominate when the B modes fell between them. The relative placement of the B modes depends, of course, on the precise length of the laser cavity, and the relative intensity of lines A and B would be a sensitive periodic function of the cavity length. The separation d between adjacent positions of maximum suppression of line B is given by

$$d = 1/2\Delta\sigma \text{ cm},$$

where $\Delta\sigma$ is the $^3P_2 - {}^3P_1$ separation in cm^{-1}. Thus, line B would be expected to pass through a maximum every 0.9 cm of traversal of one end mirror.[19]

In the course of our experiments we searched for alternations in the intensities of lines A and B as the laser cavity length was varied by several cm, but found no evidence of such behavior under our discharge conditions, neither pulsed nor cw.

VI. CONCLUSION

We have observed competition among the four fine-structure laser lines in atomic oxygen at 8446 Å. These competition effects can be explained on the basis of the interaction of laser lines oscillating on Doppler-broadened transitions sharing a common lower level. The detailed manifestations of the coupling effects may be different at lower oxygen partial pressures.

Taken as a whole, the 8446-Å oxygen laser presents a beautiful combination of interesting gas-laser phenomena.

ACKNOWLEDGMENTS

The assistance and support of Norman Knable is gratefully acknowledged. One of us (L. H. D.) wishes to thank Dr. Knable, NASA Electronics Research Center, and the National Research Council for the postdoctoral fellowship he held during this period. It is a pleasure to acknowledge the technical assistance of Eugene Leonard, helpful advice from Dr. David Burnham, and many useful discussions with Professor Ali Javan.

APPENDIX: PULSED-DISCHARGE SYSTEM

Some additional experimental information about the pulsed-discharge oxygen-argon laser may be of interest. The gain in this case is much higher

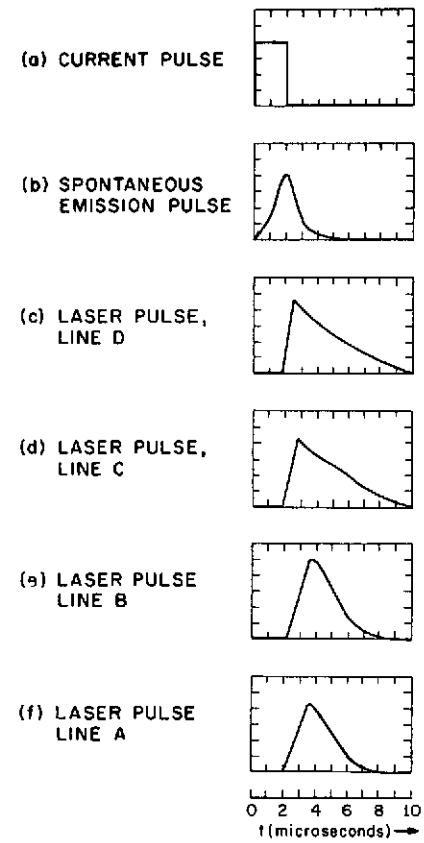

FIG. 7. Relative time dependence of current pulse, spontaneous-emission signal, and laser output from lines A, B, C, and D. The time (horizontal) axis is 1 μsec/div. The intensity (vertical) axes have all been normalized.

than for the cw case, with peak pulse powers of 250 mW (average power about 1 mW with a 2000 pulses/sec repetition rate). The intensity of the laser lines, especially of the weak pair of lines A and B, was found to be strongly dependent on the voltage, duration, and repetition rate of the current pulses, the whole behavior being highly resonant in character. Apparently, this was due to plasma resonances in the discharge tube. However, with optimum settings at a fixed pressure the four lines took on the definite intensity ratios shown in Fig. 2(a), with the A line second strongest to the D line. A cw-discharge produces slightly different ratios. Figure 6 shows interferometer traces of the four lines, comparing pulse and cw excited systems.

In order to ascertain whether or not the pulsed A, B, C, and D lines actually did occur at the same time, and so could be expected to interact via the coupled-transition mechanism as in the cw case, the following experiment was tried. The output of the pulsed laser was passed through a piezoelectrically scanned Fabry–Perot interferometer into a fast photomultiplier, which was observed on an oscilloscope triggered by the power supply pulse. The Fabry–Perot could be set manually with a dc voltage to pass the pulses from only one of the four lines at a time. The results are shown in Fig. 7. The A and B pulses lag about 1 μsec behind C and D pulses and are shorter, but they completely overlap with C and D. Reducing the gain of the D line to the level of the A or B lines changed the D-pulse time dependence to the *same* as that of A, so the difference in timing can be completely accounted for by the differences in gain of the four lines.

---

*Work supported in part by the National Aeronautics and Space Administration and NASA Electronics Research Center.

†National Academy of Sciences Postodoctoral Resident Research Associate. Present address: Maharishi International University, Rishikesh, India.

‡Present Address: Los Alamos Scientific Laboratory, Los Alamos, N. M. 87544.

[1]M. S. Feld, B. J. Feldman, A. Javan, and L. H. Domash, the preceding paper, Phys. Rev. A 1, 257 (1973).

[2]L. H. Domash, M. S. Feld, B. J. Feldman, and A. Javan, Bull. Am. Phys. Soc. 16, 593 (1971).

[3]W. R. Bennett, Jr., W. L. Faust, R. A. McFarlane, and C. K. N. Patel, Phys. Rev. Letters 8, 470 (1962).

[4]M. S. Feld, B. J. Feldman, and A. Javan, Bull. Am. Phys. Soc. 12, 669 (1967).

[5]Various aspects of the laser-induced line-narrowing effect are reviewed by M. S. Feld, in *Fundamental and Applied Laser Physics, Proceedings of the Esfahan Symposium* (Wiley, New York, 1972). Interested readers will find further discussions and reference therein.

[6]The line shape of this depletion will take the form of two superimposed Lorentzian curves of widths γ_L and γ_2.

[7]W. E. Lamb, Jr., Phys. Rev. 134, A1429 (1964).

[8]H. K. Holt, Phys. Rev. Letters 20, 410 (1968).

[9]Th. Hansch, R. Keil, A. Schubert, and P. Toschek, Z. Physik 226, 293 (1969).

[10]I. M. Beterov and V. P. Chebotayev, Zh. Eksperim. i Teor. Fiz. Pis'ma Redaktsiyu 9, 216 (1969) [Sov. Phys. JETP Letters 9, 127 (1969)].

[11]B. J. Feldman and M. S. Feld, Phys. Rev. A 5, 899 (1972).

[12]Because of the dissociative mode of production, the velocity distribution of the laser levels is much wider than that of the atomic-oxygen ground state. The lower laser levels are coupled to the ground state by uv resonance radiation. The selective reabsorption of this radiation over the central portion of the resonance lines selectively increases the populations of the lower laser levels for atoms with low velocities, thereby depleting the central portions of the fine-structure gain profiles. See Ref. 1 for full details.

[13]C. K. N. Patel, R. A. McFarlane, and W. L. Faust, Phys. Rev. 133, A1244 (1964). In this paper the oxygen lines were attributed to bromine.

[14]W. L. Wiese, M. W. Smith, and B. M. Glennon, *Atomic Transition Probabilities*, U. S. Dept. of Commerce, Natl. Bur. Std. (U.S. GPO, Washington, D.C., 1966), Vol. I.

[15]Upper-level lifetime: see, for example, J. Solarski and W. L. Wiese, Phys. Rev. 135, A1236 (1964). Lower-level lifetime: see, for example, A. B. Prag and K. C. Clark, Phys. Rev. Letters 12, 34 (1964). These and other references are contained in Ref. 14.

[16]L. W. Parker and J. R. Holmes, J. Opt. Soc. Am. 43, 103 (1953).

[17]W. R. Bennett, Jr., *Proceedings of the Third International Conference on Quantum Electronics* (Dunod Cie, Paris, New York, 1963).

[18]L. N. Tunitsky and E. M. Cherkasov, J. Opt. Soc. Am. 56, 1783 (1966); Opt. i Spektroskopiya 23, 287 (1967) [Opt. Spectry. 23, 154 (1967)].

[19]Behavior of this type was first discussed by M. S. Feld, Ph. D. thesis (MIT, 1967) (unpublished).